HHS Public Access

Author manuscript

Neuropharmacology. Author manuscript; available in PMC 2022 June 01.

Published in final edited form as:

Neuropharmacology. 2021 June 01; 190: 108565. doi:10.1016/j.neuropharm.2021.108565.

Activation of V_{1a} Vasopressin Receptors Excite Subicular Pyramidal Neurons by Activating TRPV1 and Depressing GIRK Channels

Saobo Lei[#], **Binqi Hu**, **Neda Rezagholizadeh**

Department of Biomedical Sciences, School of Medicine and Health Sciences, University of North Dakota, Grand Forks, ND58203, USA

Abstract

Arginine vasopressin (AVP) is a nonapeptide that serves as a neuromodulator in the brain and a hormone in the periphery that regulates water homeostasis and vasoconstriction. The subiculum is the major output region of the hippocampus and an integral component in the networks that processes sensory and motor cues to form a cognitive map encoding spatial, contextual, and emotional information. Whereas the subiculum expresses high densities of AVP-binding sites and AVP has been shown to increase the synaptic excitability of subicular pyramidal neurons, the underlying cellular and molecular mechanisms have not been determined. We found that activation of V_{1a} receptors increased the excitability subicular pyramidal neurons via activation of TRPV1 channels and depression of the GIRK channels. V_{1a} receptor-induced excitation of subicular pyramidal neurons required the function of phospholipase Cβ, but was independent of intracellular Ca^{2+} release. Protein kinase C was responsible for AVP-mediated depression of GIRK channels, whereas degradation of phosphatidylinositol 4,5-bisphosphate was involved in V_{1a} receptor-elicited activation of TRPV1 channels. Our results may provide one of the cellular and molecular mechanisms to explain the physiological functions of AVP in the brain.

Graphical Abstract

[#]**Corresponding author:** Saobo Lei (saobo.lei@und.edu).

Authors contributions: All the experiments were performed in the University of North Dakota. S.L. conceived and designed the study. S. L., B. H. and N. R. performed experiments, analyzed data and prepared figures. S. L. wrote and revised the manuscript. All authors approved the final version of the manuscript. All authors agree to be accountable for all aspects of the work in ensuring that questions related to the accuracy or integrity of any part of the work are appropriately investigated and resolved. All persons designated as authors qualify for authorship, and all those who qualify for authorship are listed.

Declarations of interest: no

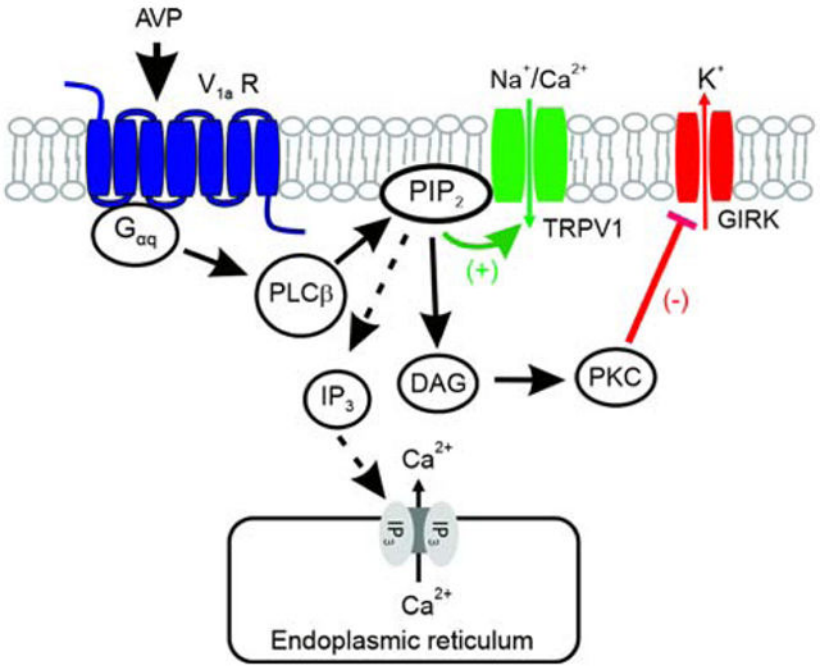

Keywords

excitability; action potential; K^+ channels; cation channel; G protein; subiculum; peptide; synapse; receptor

1. Introduction

The neurosecretory cells in the paraventricular and supraoptic nuclei of the hypothalamus synthesize two important hormones: arginine vasopressin (AVP) (also known as antidiuretic hormone) and oxytocin. After synthesis in the hypothalamus, these hormones are transported along the axons of these neurosecretory cells to the posterior pituitary where they are released into the blood stream to play their traditional physiological functions on blood vessels, kidney and uterus (Stoop, 2012). In addition to these neurosecretory functions, AVP and oxytocin also travel along the axonal projections from parvocellular neurons of the hypothalamus to discrete extrahypothalamic limbic brain regions including the hippocampus, subiculum, amygdala and nucleus accumbens (Buijs, 1978; Buijs and Swaab, 1979; DeVries et al., 1985; Hawthorn et al., 1985; Lang et al., 1983). Whereas the hypothalamus is the major source of AVP and oxytocin in the brain, AVP immunoreactivity has also been detected in neurons in the extrahypothalamic structures including the bed nucleus of stria terminalis, septal region, medial amygdala and locus coeruleus (Caffe and van Leeuwen, 1983; Sofroniew, 1985; van Leeuwen and Caffe, 1983) (for a review see (Cilz et al., 2019)). Similar to AVP, neuronal expression of oxytocin has also been found in medial amygdaloid nucleus and the cell group near the anterior commissure extending into the bed nucleus of stria terminalis (Otero-Garcia et al., 2016). Whereas oxytocin interacts primarily with the oxytocin receptors, AVP functions by interacting with 3 types of vasopressin receptors: V_{1a}, V_{1b} and V_2 receptors. Whilst V_2 receptors are coupled to G_s proteins

resulting in increased activity of adenylyl cyclase to elevate cyclic AMP level, V_{1a} and V_{1b} receptors are coupled to $G_{q/11}$ proteins enhancing the activity of phospholipase Cβ (PLCβ) which hydrolyses phosphatidylinositol 4,5-bisphosphate (PIP_2) to generate 1,4,5-trisphosphate (IP_3) to increase intracellular Ca^{2+} release and diacylglycerol (DAG) to activate protein kinase C (PKC). In addition to its hormonal roles in constricting blood vessels and decreasing urine volume, AVP is also a neuromodulator that regulates a diverse range of functions including anxiety (Caldwell et al., 2008; Neumann and Landgraf, 2012), social behaviors (Cilz et al., 2019; Kompier et al., 2019), learning and memory (Caldwell et al., 2008; de Wied et al., 1993), nociception (Koshimizu and Tsujimoto, 2009) and circadian rhythms (Gizowski et al., 2017). However, the cellular and molecular mechanisms whereby AVP modulates these physiological functions and pathological disorders are not fully determined.

The subiculum is the major output region of the hippocampus and targets a variety of cortical and subcortical areas (O'Mara et al., 2001). Together with CA1 pyramidal neurons, the subiculum processes sensory and motor cues to form a cognitive map encoding spatial, contextual, and emotional information, which is then transmitted throughout the brain. Subiculum is therefore an integral component in the networks underlying memory for spatial tasks (O'Mara et al., 2001). In the subiculum, high densities of AVP-binding sites have been detected (Cilz et al., 2019; Insel et al., 1994; Phillips et al., 1988) and AVP increases the synaptic excitability of subiculum neurons (Chepkova et al., 1995). However, the precise actions of AVP and its underlying cellular and molecular mechanisms in the subiculum have not been determined. In the present study, we probed the effects of AVP on the excitabilities of the pyramidal neurons in the subiculum. Our results demonstrate that AVP enhanced the excitabilities of pyramidal neurons via V_{1a} receptor-mediated activation TRPV1 channels and depression of the G protein-gated inwardly rectifying potassium (GIRK) channels. AVP-elicited excitation of subicular pyramidal neurons required the function of PLCβ but was independent of intracellular Ca^{2+} release. PKC was responsible for AVP-mediated depression of GIRK channels, whereas PIP_2 depletion was involved in V_{1a} receptor-induced activation of TRPV1 channels. Our results may provide one of the cellular and molecular mechanisms to explain the physiological functions of AVP *in vivo*.

2. Materials and Methods

2.1. Slice preparation

Horizontal brain slices (300 μm) were prepared from both male and female Sprague-Dawley rats (20–28 days old) purchased from Envigo RMS, INC. (Indianapolis, IN), TRPV1 knockout (KO) mice (B6.129X1-*Trpv1*^{tm1Jul}/J, strain 003770, 1–2 months) and the corresponding age-matched wild-type (WT) mice (C57BL/6J, strain 000664) purchased from The Jackson Laboratory. All animals were housed in the Center for Biomedical Research in the University of North Dakota with food and water available *ad libitum*. The animal rooms were maintained on a 14/10 h light–dark cycle (lights on at 7:00 a.m.), with a room temperature of 22°C. All procedures and experiments presented in this study were approved by the Institutional Animal Use and Care Committee of the University of North Dakota and performed in accordance with the National Institutes of Health Guide for the

Care and Use of Laboratory Animals (NIH Publications No. 8023, revised 1978). The number of males and females for each experiment was kept as equal as possible. After being deeply anesthetized with isoflurane, animals were decapitated and their brains were dissected out in ice-cold saline solution that contained (in mM) 130 N-methyl-D-glucamine (NMDG)-Cl, 24 $NaHCO_3$, 3.5 KCl, 1.25 NaH_2PO_4, 0.5 $CaCl_2$, 5.0 $MgCl_2$, and 10 glucose, saturated with 95% O_2 and 5% CO_2 (pH 7.4, adjusted with HCl). Slices were then incubated in the above solution except NMDG-Cl was replaced with NaCl at 35°C for 1 hour for recovery and kept at room temperature (~22°C) until use.

2.2. Recordings of action potentials, resting membrane potentials and holding currents from subicular pyramidal neurons

Whole-cell recordings using a Multiclamp 700B amplifier (Molecular Devices, Sunnyvale, CA) in current- or voltage-clamp mode were made from the pyramidal neurons in the subiculum visually identified with infrared video microscopy (Olympus BX51WI) and differential interference contrast optics. During recordings, the bath temperature was maintained at 33–34°C by an in-line heater and an automatic temperature controller (TC-324C, Warner Instruments), unless stated otherwise. The recording electrodes were filled with (in mM) 100 K^+-gluconate, 8 KCl, 2 $MgCl_2$, 40 HEPES, 0.6 EGTA, 2 $ATPNa_2$, 0.4 GTPNa, and 7 phosphocreatine (pH 7.3), unless stated otherwise. The extracellular solution comprised (in mM) 130 NaCl, 24 $NaHCO_3$, 3.5 KCl, 1.25 NaH_2PO4, 2.5 $CaCl_2$, 1.5 $MgCl_2$ and 10 glucose, saturated with 95% O_2 and 5% CO_2 (pH 7.4). Data were filtered at 2 kHz, digitized at 10 kHz, acquired on-line and analyzed after-line using pCLAMP 10.7 software (Molecular Devices, Sunnyvale, CA). After the formation of whole-cell configuration, we routinely injected currents from −100 pA to 400 pA (duration: 400 ms) at a step of 50 pA with an interval of 10 s/injection to identify the recorded neurons. Bursting cells (BCs) fire an early burst of 2–4 action potentials (APs) upon injection of depolarizing current of threshold intensity, whereas in regular firing cells (RCs), prolonged depolarization causes either a single AP or trains of single spikes (Hu et al., 2017; Mason, 1993; Mattia et al., 1993). AVP was dissolved in the extracellular solution and bath-applied to the slice. To avoid potential desensitization induced by repeated applications of the agonist, one slice was limited to only one application of AVP. Resting membrane potentials (RMPs) and holding currents (HCs) at −60 mV were recorded in the extracellular solution supplemented with TTX (0.5 μM), kynurenic acid (1 mM) and picrotoxin (100 μM) to block AP firing, glutamatergic and GABAergic transmission, respectively. Pharmacological inhibitors were applied to the cells either extracellularly or intracellularly via the recording pipettes. For extracellular application, slices were pretreated for at least 2 hours to ensure permeation of reagents into the cells in the slices and the extracellular solution continuously contained the same concentration of the reagents, unless stated otherwise. For intracellular application, we waited for >15 min after the formation of whole-cell configuration to ensure the diffusion of the inhibitors into the cells. For the experiments with TRPV1 KO mice and the corresponding WT mice, the experimenters were blind to the identities of the mice.

2.3. Data analysis

Data are presented as the means ± S.E.M. *N* numbers in the text were the numbers of cells used for each experiment. To minimize potential influences of variation from individual

animals, at least 4 animals were used for each experiment. Because the maximal response occurred within 5 min during the application of AVP, we measured the peak response of AVP for statistical analysis. The control data for AVP-induced inward currents were pooled results from the control experiments performed for each individual pharmacological experiment. One-way ANOVA followed by Tukey's or Dunnett's multiple comparisons test was used for statistical analysis when the pooled control data were used for comparison. Mann-Whitney test or Wilcoxon matched-pairs signed rank test (abbreviated as Wilcoxon test in the text) or Two-way repeated measures ANOVA followed by Sidak multiple comparison test was used for statistical analysis as appropriate; *P* values were reported throughout the text and significance was set as $P < 0.05$.

2.4. Chemicals

The following chemicals were products of R&D Systems: AVP, tetrodotoxin (TTX), kynurenic acid, picrotoxin, SR49059, TASP0390325, tolvaptan, GDP-β-S, U73122, U73343, heparin, thapsigargin, chelerythrine, bisindolylmaleimide II (Bis II), KB-R7943, capsazepine, AMG9810, AMG1629, capsaicin, ML 133, ML 297 and SCH23390. Dioctanoyl phosphatidylinositol 4,5-bisphosphate (dic8-PIP_2) was purchased from Echelon Biosciences. Drugs were initially prepared in stock solution, aliquoted and stored at −20°C. For those chemicals requiring dimethyl sulfoxide (DMSO) as a solvent, the concentration of DMSO was less than 0.1%. This concentration of DMSO either in the recording pipettes or in the bath had no significant effects on neuronal activity.

3. Results

3.1. AVP excites both bursting cells and regular firing cells in the subiculum

Whereas the subiculum has been shown to express AVP-binding sites (Cilz et al., 2019; Insel et al., 1994; Phillips et al., 1988) and bath application of AVP enhances synaptic excitabilities of subicular pyramidal neurons (Chepkova et al., 1995), the precise actions of AVP in subicular pyramidal neurons have not been elucidated. We probed the effects of AVP on the excitabilities of the principal neurons in the subiculum by recording the resting membrane potential (RMP) and potential appearance of action potential (AP) firing from the subicular pyramidal neurons in slices. Subiculum was distinguished from bordering regions by the diffuse distribution of pyramidal cells, compared to the tightly packed pyramidal cell layer of CA1, and the lack of distinct cortical layers observed in the entorhinal cortex (Hu et al., 2017). The extracellular solution contained kynurenic acid (1 mM) to block glutamatergic transmission and picrotoxin (100 μM) to block GABAergic transmission. Under these circumstances, the effects of AVP should be from the recorded neurons. For better comparisons, we used AVP at 0.3 μM which is a near-saturating concentration of AVP (Ramanathan et al., 2012) for each experiment. Because there are two types of pyramidal neurons, i.e., bursting cells (BCs) and regular firing cells (RCs) in the subiculum according to their firing patterns (Graves et al., 2012; Hu et al., 2017; Wozny et al., 2008), we identified the neuronal types by injecting negative and positive currents into the recorded cells initially (Fig. 1). BCs fire an early burst of 2–4 APs upon injection of depolarizing current of threshold intensity, whereas in RCs, prolonged depolarization causes either a single AP or trains of single spikes (Mason, 1993; Mattia et al., 1993). The possible reason

for the bursting property of BCs is their selective expression of Cav3.1-containing T-type Ca^{2+} channels (Joksimovic et al., 2017). Of the 40 cells recorded, 28 cells were classified as BCs (~70%) and 12 cells were categorized as RCs (~30%), as reported previously (Mason, 1993; Mattia et al., 1993). We then recorded the RMPs and APs in response to AVP in both cell types. Out of the 28 BCs recorded, 17 cells (~61%) showed transient AP firing (263 ± 33 APs/min, n = 17, $P < 0.0001$, Fig. $1A_1$–A_3) in response to bath application of AVP, whereas 11 BCs (~39%) displayed a subthreshold depolarization (Control: −63.5 ± 1.5 mV, AVP: −60.1 ± 1.5 mV, net depolarization: 3.4 ± 0.4 mV, n = 11, $P = 0.001$, Fig. $1A_4$–A_5). Of the 12 RCs recorded, 6 cells (~50%) demonstrated transient AP firing (297 ± 97 APs/min, n = 6, $P = 0.03$, Fig. $1B_1$–B_3) in response to bath application of AVP, whereas the remaining 6 RCs (~50%) displayed a subthreshold depolarization (Control: −61.9 ± 1.1 mV, AVP: −58.3 ± 0.9 mV, net depolarization: 3.6 ± 0.6 mV, n = 6, $P = 0.03$, Fig. $1B_4$–B_5). There were no significant differences for the AVP-elicited AP-firing ($P = 0.85$) and subthreshold depolarization ($P = 0.66$) between BCs and RCs.

Because application of AVP elicited only subthreshold depolarization in at least 50% subicular pyramidal neurons, we then assessed the effect of AVP on neuronal excitability by injecting a serious of incremental positive currents (from 30 pA to 480 pA, at an interval of 30 pA with a duration of 600 ms) before and during the application of AVP (Fig. 2). Application of AVP significantly increased the number of APs recorded from both BCs (n = 12, $F_{(1,11)} = 125.9$, $P < 0.0001$, Two-way repeated measures ANOVA followed by Sidak multiple comparison test, Fig. $2A_1$–A_2) and RCs (n = 6, $F_{(1,5)} = 9.71$, $P = 0.026$, Two-way repeated measures ANOVA followed by Sidak multiple comparison test, Fig. $2B_1$–B_2), further supporting the notion that AVP excites both BCs and RCs in the subiculum.

The above experiments were performed in the extracellular solution containing kynurenic acid (1 mM) to block glutamatergic transmission and picrotoxin (100 μM) to block GABAergic transmission. However, in physiological condition, both glutamatergic transmission and GABAergic transmission are functional. We therefore repeated the experiments in the normal extracellular solution without adding any blockers. Under these circumstances, application of AVP still significantly enhanced the number of APs elicited by the positive current injection protocol in both BCs (n = 16, $F_{(1,15)} = 69.85$, $P < 0.0001$, Two-way repeated measures ANOVA followed by Sidak multiple comparison test, Fig. $2C_1$–C_2) and RCs (n = 8, $F_{(1,7)} = 23.96$, $P = 0.002$, Two-way repeated measures ANOVA followed by Sidak multiple comparison test, Fig. $2D_1$–D_2). These results suggest that AVP-mediated increases in AP firing frequency should be physiologically functional. Because the effects of AVP in the subiculum were not cell-specific, we used both cell types for the remaining experiments.

3.2. AVP-mediated excitation of subicular pyramidal neurons is mediated by V_{1a} receptors

We then used voltage clamp and recorded holding currents at −60 mV in the abovementioned extracellular solution supplemented with TTX (0.5 μM) to further block AP firing. Under these circumstances, application of AVP induced an inward current (−55.1 ± 9.6 pA, n = 14, $P = 0.0001$, Fig. 3A, 3E). We denoted the AVP-induced inward currents in

control condition as I_{AVP} thereafter. We tested the roles of AVP receptors in AVP-induced excitation of subicular pyramidal neurons. Pretreatment of slices with and continuous bath application of the selective V_{1a} receptor antagonist, SR49059 (1 μM), completely blocked I_{AVP} (−1.9 ± 1.8 pA, n = 10, P = 0.49 vs. baseline, Fig. 3B, 3E), demonstrating the involvement of V_{1a} receptors. Conversely, I_{AVP} was not significantly altered by application of the selective V_{1b} antagonist, TASP0390325 (TASP, 0.5 μM, −58.5 ± 4.8 pA, n = 11, P = 0.001 vs. baseline; P = 0.47 vs. control I_{AVP}, Fig. 3C, 3E) or the selective V_2 receptor antagonist, tolvaptan (50 nM, −54.7 ± 10.5 pA, n = 6, P = 0.03 vs. baseline; P = 0.97 vs. control I_{AVP}, Fig. 3D–E). These results together demonstrate that AVP-induced excitation of subicular pyramidal neurons is mediated by activation of V_{1a} receptors.

3.3. AVP-elicited excitation of subicular pyramidal neurons is mediated by activation of a cationic conductance and depression of an inwardly rectifying K^+ channel

We examined the ionic mechanisms underlying AVP-induced excitation of subicular pyramidal neurons by constructing the current-voltage (I-V) relationship of the currents generated by AVP. The abovementioned extracellular solution contained TTX (0.5 μM) to block voltage-gated Na^+ channels. Cells were held at −60 mV and stepped from −120 mV to −40 mV for 400 ms at a voltage interval of 10 mV every 5 s. Steady-state currents were measured within 5 ms prior to the end of the step voltage protocol. In 12 of the 20 cells recorded, AVP elicited a persistent inward current at the voltage range between −120 mV and −40 mV (Fig. $4A_1$–A_3), suggestive of the involvement of cation channels (Fig. $4A_3$). The I-V curve of the I_{AVP} in the remaining 8 cells resembled that of the inwardly rectifying K^+ (Kir) channels with a reversal potential of −85.0 ± 4.7 mV (n = 8, Fig. $4B_1$–B_3), close to the calculated K^+ reversal potential (−90.3 mV). These results demonstrate that activation of V_{1a} receptors excites ~60% (12/20) subicular pyramidal neurons primarily by activating a cationic conductance and ~40% (8/20) subicular pyramidal neurons mainly by depressing a Kir channel. AVP-elicited activation of cation channels and depression of K^+ channels were not correlated with the neuronal types in the subiculum, because the 12 cells showing an I-V of cation channels included 8 BCs and 4 RCs whereas the 8 cells displaying an I-V of Kir channels consisted of 6 BCs and 2 RCs.

Because micromolar concentration of Ba^{2+} (100–300 μM) has been shown to block Kir channels by at least 80% (Hu et al., 2017; Lacey et al., 1988; Li et al., 2019), we included 300 μM Ba^{2+} in the extracellular solution to inhibit Kir channels. Bath application of 300 μM Ba^{2+} by itself induced an inward current (−40.6 ± 6.2 pA, n = 12, P < 0.001 vs. baseline, Fig. $4C_1$–C_2) and the I-V curve of the Ba^{2+}-induced net currents showed inward rectification (n = 5, Fig. $4C_3$), suggesting that subicular pyramidal neurons express Kir channels. In the presence of Ba^{2+}, application of AVP induced a significantly smaller inward current (−23.0 ± 3.4 pA, n = 12, P < 0.001 vs. baseline; P = 0.006 vs. control I_{AVP}, Fig. $4C_1$–C_2), further confirming the involvement of Kir channels. We further extended the voltage range from −120 mV to +40 mV to measure the reversal potential of the cationic currents elicited by AVP in the continuous presence of Ba^{2+} (300 μM) to block the contamination of the Kir channels. In addition to 300 μM $BaCl_2$, the extracellular solution also contained TTX (0.5 μM) to block voltage-gated Na^+ channels, $CdCl_2$ (200 μM) and $NiCl_2$ (1 mM) to block the contamination of voltage-gated Ca^{2+} channels. Under these circumstances, AVP-elicited net

currents showed a reversal potential of −15.9 ± 1.5 mV with outward rectification (n = 11, Fig. 4D$_1$–D$_3$), further confirming the involvement of cationic channels.

3.4. TRPV1 channels are necessary for AVP-mediated excitation of subicular pyramidal neurons

Na^+/Ca^{2+} exchanger moves 3 Na^+ ions in and 1 Ca^{2+} ion out, therefore generating an electrogenic potential. We therefore tested whether AVP excites subicular pyramidal neurons by increasing the function of Na^+/Ca^{2+} exchanger. Pretreatment of slices with and continuous bath application of the selective Na^+/Ca^{2+} exchanger inhibitor, KB-R7943 (70 μM), did not significantly alter I_{AVP} (−47.6 ± 7.7 pA, n = 10, P = 0.002 vs. baseline; P = 0.93 vs. control I_{AVP}, Fig. 5A, 5C), suggesting that the functions of Na^+/Ca^{2+} exchangers are not involved in AVP-induced excitation of subicular pyramidal neurons.

The I-V curve of AVP-sensitive currents in the presence of Ba^{2+} to block the contamination of Kir channels showed outward rectification (Fig. 4D$_3$), resembling that of TRPV1 channels (Wu et al., 2010). Because TRPV1 channels are sensitive to temperature and the recording temperature in the current study was at 33–34°C, we therefore recorded I_{AVP} at room temperature (22–23°C). Application of AVP at room temperature induced a much smaller inward current (−9.3 ± 2.5 pA, n = 13, P < 0.001 vs. baseline; P < 0.0001 vs. control I_{AVP}, Fig. 5B–C), demonstrating that AVP-elicited inward currents are temperature-dependent. We further probed the roles of TRPV1 channels in AVP-mediated excitation of subicular pyramidal neurons. Bath application of the TRPV1 blocker, capsazepine (10 μM), significantly reduced I_{AVP} (−18.5 ± 4.6 pA, n = 11, P = 0.002 vs. baseline; P = 0.002 vs. control I_{AVP}, Fig. 5D, 5J). Co-application of capsazepine with Ba^{2+} (300 μM) to block Kir channels annulled I_{AVP} (0.15 ± 0.54 pA, n = 11, P = 0.78 vs. baseline, Fig. 5E, 5J), suggesting that TRPV1 and Kir channels are the two principal conductances involved in AVP-induced excitation of subicular pyramidal neurons. Furthermore, I_{AVP} was significantly reduced by bath applications of other two TRPV1 blockers, AMG9810 (10 μM, −29.0 ± 3.9 pA, n = 12, P = 0.0001 vs. baseline; P = 0.02 vs. control I_{AVP}, Fig. 5F, 5J) and AMG21629 (3 μM, −25.0 ± 2.8 pA, n = 10, P = 0.002 vs. baseline; P = 0.009 vs. control I_{AVP}, Fig. 5G, 5J), suggesting the involvement of TRPV1 channels. If TRPV1 channels are required for AVP-elicited excitation, application of the TRPV1 agonist, capsaicin, should elicit an inward current in the subicular pyramidal neurons. Consistent with our anticipation, bath application of capsaicin (50 μM) elicited an inward current in the subicular pyramidal neurons (−69.3 ± 3.8 pA, n = 6, P = 0.03 vs. baseline, Fig. 5H, 5J) and co-application of capsazepine blocked capsaicin-induced inward currents (1.20 ± 0.92 pA, n = 8, P = 0.23 vs. baseline, Fig. 5I–J), further confirming the expression of TRPV1 channels in the subiculum. Consistent with the results of the pharmacological experiments, application of AVP elicited a significantly smaller inward current in slices cut from TRPV1 KO mice (−10.4 ± 2.2 pA, n = 21, Fig. 5K, 5P), compared with the WT mice (−46.6 ± 5.8 pA, n = 15, P < 0.0001, Fig. 5L, 5P). Moreover, application of capsaicin elicited an inward current recorded from subicular pyramidal neurons in slices cut from WT mice (−59.1 ± 6.9 pA, n = 12, P = 0.0005, Fig. 5M, 5P), but failed to evoke inward currents in slices cut from TRPV1 KO mice (0.45 ± 1.77 pA, n = 12, P = 0.85, Fig. 5N, 5P). In the slices cut from TRPV1 KO mice, co-application of Ba^{2+} (300 μM) blocked AVP-induced inward currents (−0.64 ± 2.01 pA, n = 12, P = 0.79,

Fig. 5O–P). These data together indicate that activation of V_{1a} receptors excites subicular pyramidal neurons by activating TRPV1 channels and depressing Kir channels.

3.5. GIRK channels are involved in AVP-elicited excitation of subicular pyramidal neurons

We further characterized the subtypes of the Kir channels involved in AVP-induced excitation. There are seven Kir channel subfamilies that can be classified into four functional groups: i) Kir2 subfamily comprising Kir2.1, Kir2.2, Kir2.3 and Kir2.4 form the classical Kir channels and are constitutively active; ii) Kir3 subfamily including Kir3.1 (GIRK1), Kir3.2 (GIRK2), Kir3.3 (GIRK3) and Kir3.4 (GIRK4) encoded by the genes KCNJ3, KCNJ6, KCNJ9, and KCNJ5, respectively, constitute the G protein-gated GIRK channels; iii) Kir6 subfamily encompassing Kir6.1 and Kir6.2 form the ATP-sensitive K^+ (K_{ATP}) channels; iv) K^+ transport channels include Kir1.1, Kir4.1, Kir4.2 and Kir7.1 (Hibino et al., 2010). Whereas AVP has been shown to depress K_{ATP} channels (Shi et al., 2007; Wakatsuki et al., 1992), K_{ATP} channels are unlikely to be involved because our recording solution in the pipettes contained 2 mM ATP which blocked K_{ATP} channels. We used ML 133, a specific antagonist for Kir2 subfamily (Ford and Baccei, 2016; Huang et al., 2018; Kim et al., 2015; Sonkusare et al., 2016; Wang et al., 2011) to test the roles of the Kir2 subfamily in AVP-elicited excitation of subicular pyramidal neurons. Bath application of ML 133 (30 μM) by itself did not change the holding currents significantly (−4.6 ± 3.1 pA, n = 14, $P = 0.24$, Fig. 6A). In the presence of ML 133, application of AVP still elicited a comparable inward current (−50.3 ± 11.1 pA, n = 14, $P < 0.0001$ vs. baseline; $P = 0.73$ vs. control I_{AVP}, Fig. 6A, 6E), suggesting that Kir2 subfamily is not the Kir channels involved in AVP-elicited excitation. We then tested the roles of GIRK (Kir3) subfamily in AVP-elicited excitation. Application of SCH23390 (20 μM), a GIRK channel inhibitor (Chee et al., 2011; Kuzhikandathil and Oxford, 2002), induced an inward current by itself (−24.4 ± 3.8 pA, n = 13, $P = 0.0002$, Fig. 6B), suggesting the expression of GIRK channels in the subicular pyramidal neurons. In the continuous presence of SCH23390, application of AVP induced a significantly smaller inward current (−24.0 ± 2.8 pA, n = 13, $P = 0.0002$ vs. baseline; $P = 0.02$ vs. control I_{AVP}, Fig. 6B, 6E), suggesting that GIRK channels are involved in AVP-mediated excitation of subicular pyramidal neurons. Furthermore, co-application of SCH23390 (20 μM) and capsazepine (10 μM) blocked I_{AVP} (−3.7 ± 1.9 pA, n = 12, $P = 0.13$ vs. baseline; $P < 0.001$ vs. control I_{AVP}, Fig. 6C, 6E). Consistent with the involvement of GIRK channels, application of ML 297 (10 μM), an activator of GIRK1-containing channels (Kaufmann et al., 2013), induced an outward current (58.7 ± 10.2 pA, n = 12, $P = 0.0005$, Fig. 6D–E), suggesting that GIRK1 channels are functionally expressed in the subiculum and they may be involved in AVP-elicited excitation of subicular pyramidal neurons.

3.6. AVP-mediated excitation of subicular pyramidal neurons requires the functions of G proteins and PLCβ, but is independent of intracellular Ca^{2+} release

Because V_{1a} receptors are coupled to $G\alpha_{q/11}$, we next examined the roles of G proteins in AVP-induced excitation of subicular pyramidal neurons. Intracellular application of the G protein inactivator, GDP-β-S (0.5 mM), via the recording pipettes significantly reduced I_{AVP} (−6.4 ± 1.5 pA, n = 12, $P = 0.003$ vs. baseline; $P < 0.0001$ vs. control I_{AVP}, Fig. 7A, F), demonstrating that G proteins are required for AVP-induced excitation of subicular pyramidal neurons. Activation of V_{1a} receptors increases the function of PLCβ resulting in

the hydrolysis of PIP_2 to generate IP_3 to increase intracellular Ca^{2+} release and DAG to activate PKC. We next examined the roles of this pathway in AVP-elicited excitation of subicular pyramidal neurons. Slices were pretreated with the selective PLCβ inhibitor, U73122 (5 μM), for >2 h. The same concentration of the inactive analog U73343 was used as a control. Under these circumstances, application of AVP induced a significantly smaller I_{AVP} in the slices treated with U73122 (−12.1 ± 3.2 pA, n = 15, $P = 0.004$, Fig. 7B, 7F), compared with the slices pretreated with U73343 (−59.0 ± 7.4 pA, n = 12, $P < 0.001$ vs. baseline; $P < 0.001$ vs. U73122, Fig. 7C, F). These results demonstrate that the function of PLC is required for AVP-elicited excitation of subicular pyramidal neurons.

We further tested the roles of intracellular Ca^{2+} release in AVP-elicited excitation of subicular pyramidal neurons. Application of the IP_3 receptor blocker, heparin (2 mg/ml), via the recording pipettes, failed to significantly alter I_{AVP} (−52.5 ± 5.7 pA, n = 12, $P < 0.001$ vs. baseline; $P = 0.90$ vs. control I_{AVP}, Fig. 7D, F), suggesting that IP_3 receptors are not required for AVP-induced increases in neuronal excitability in the subiculum. Likewise, intracellular application of the sarco-endoplasmic reticulum Ca^{2+}-ATPase inhibitor, thapsigargin (10 μM), via the recording pipettes did not significantly change I_{AVP} (−56.1 ± 10.4 pA, n = 12, $P < 0.001$ vs. baseline; $P = 0.94$ vs. control I_{AVP}, Fig. 7E–F). These results demonstrate that intracellular Ca^{2+} release is not required for AVP-induced excitation of subicular pyramidal neurons.

3.7. PKC is required for the depression of GIRK channels

We tested the roles of PKC in AVP-mediated excitation of subicular pyramidal neurons. Pretreatment of slices with the selective PKC inhibitor, chelerythrine (10 μM), significantly reduced I_{AVP} (−26.4 ± 3.2 pA, n = 17, $P < 0.0001$ vs. baseline; $P < 0.001$ vs. control I_{AVP}, Fig. 8A, 8E). Similarly, pretreatment of slices with bisindolylmaleimide II (Bis II, 1 μM), another PKC inhibitor, significantly reduced I_{AVP} (−29.0 ± 3.2 pA, n = 12, $P = 0.0005$ vs. baseline; $P < 0.01$ vs. control I_{AVP}, Fig. 8B, 8E). Whilst application of the PKC inhibitors significantly reduced AVP-induced inward currents, there was a large amount of current resistant to PKC inhibition. Because our results demonstrated that V_{1a} receptor activation excited subicular pyramidal neurons by activating TRPV1 channels and depressing GIRK channels, we further probed which type of channels is the target for PKC. We included 20 μM SCH23390 in the extracellular solution to block GIRK channels. In the presence of SCH23390, AVP-induced inward currents should be mediated by TRPV1 channels. Nonetheless, AVP-induced inward currents in the presence of both SCH23390 and Bis II were not significantly different from those when Bis II was applied alone ($P > 0.05$, Fig. 8C, E), suggesting that GIRK channels are the target for PKC. We used the TRPV1 KO mice to further probe the target of PKC. Application of Bis II completely blocked AVP-induced inward currents in slices cut from TRPV1 KO mice (0.19 ± 1.75 pA, n = 12, $P = 0.91$ vs. baseline, Fig. 8D–E), which is significantly smaller compared with the control effect of AVP in TRPV1 KO mice ($P = 0.001$, Fig. 8E). These data together demonstrate that the PKC target is GIRK channels.

3.8. Degradation of PIP_2 is involved in V_{1a} receptor-elicited activation of TRPV1 channels in subicular pyramidal neurons

Because PLCβ-mediated depletion of PIP_2 has been demonstrated to be a mechanism underlying the modulation of numerous ion channels (Rodriguez-Menchaca et al., 2012; Suh and Hille, 2008), we next probed the roles of PIP_2 depletion induced by activation of PLCβ. Inclusion of the short-chain, water-soluble analog dioctanoyl (dic8)-PIP_2 (20 μM) in the recording pipettes significantly reduced AVP-induced inward currents (−6.4 ± 3.9 pA, n = 18, $P < 0.0001$ vs. baseline; $P < 0.001$ vs. control I_{AVP}, Fig. 9A, D), suggesting that PIP_2 depletion is involved in AVP-mediated excitation of subicular pyramidal neurons. We further tested whether PIP_2 depletion is involved in V_{1a} receptor-mediated activation of TRPV1 channels or depression of GIRK channels. Bath application of AVP did not elicit significant inward currents when SCH23390 was included in the extracellular solution to block GIRK channels and dic8-PIP_2 was included in the intracellular solution to compensate for PIP_2 depletion (−0.92 ± 0.82 pA, n = 16, $P = 0.35$ vs. baseline, Fig. 9B, 9D), which was significantly smaller compared with the effect of AVP when dic8-PIP_2 was applied intracellularly alone ($P < 0.01$, Fig. 9D). Nevertheless, intracellular perfusion of dic8-PIP_2 failed to further reduce AVP-elicited inward currents in slices cut from TRPV1 KO mice (−11.7 ± 1.8 pA, n = 18, $P < 0.0001$ vs. baseline; $P = 0.79$ vs. AVP alone, Fig. 9C–D). These results collectively demonstrate that PIP_2 depletion is responsible for V_{1a} receptor-mediated activation of TRPV1 channels.

4. Discussion

Our results demonstrate that activation of V_{1a} receptors increases the excitability of pyramidal neurons in the subiculum by activation of TRPV1 channels and inhibition of GIRK channels. The V_{1a} receptor-elicited excitation of subicular pyramidal neurons is mediated by activation of PLCβ but independent of intracellular Ca^{2+} release. PKC is required for V_{1a} receptor-mediated depression of GIRK channels, whereas PIP_2 depletion is involved in V_{1a} receptor-elicited activation of TRPV1 channels. Our results may therefore provide one of the cellular and molecular mechanisms to explain the physiological functions of AVP *in vivo*.

We found that in about 60% of the subicular pyramidal neurons activation of V_{1a} receptors increases neuronal excitability primarily by activating TRPV1 channels. TRPV1 channels showed outward rectification (Wu et al., 2010) and the I-V curve of the AVP-elicited currents displayed outward rectification. The involvement of TRPV1 channels was further supported by the pharmacological experiments because application of the TRPV1 channel blockers significantly reduced AVP-elicited currents. Moreover, application of AVP induced a significantly smaller current in slices cut from TRPV1 KO mice compared with wild-type mice.

How does activation of V_{1a} receptors result in opening of TRPV1 channels? V_{1a} receptors are coupled to $G_{q/11}$ resulting in increases in the function of PLCβ which hydrolyses PIP_2 to generate IP_3 to elevate intracellular Ca^{2+} release and DAG to activate PKC. Our results demonstrate that V_{1a} receptor-mediated excitation of subicular pyramidal neurons requires the function of PLCβ, but is independent of intracellular Ca^{2+} release. We further

demonstrate that PIP_2 depletion is responsible for V_{1a} receptor-elicited activation of TRPV1 channels. Consistent with our results, TRPV1 channels are activated by many $G\alpha_q$-coupled receptors including oxytocin receptors (Hu et al., 2020a), bradykinin receptor 2 (Shin et al., 2002), prostaglandin receptor (Moriyama et al., 2005), protease activated receptor 2 (Amadesi et al., 2004), histamine receptor 1 (Shim et al., 2007), endothelin-1 receptors (Plant et al., 2007), neurokinin receptors (Sculptoreanu et al., 2008; Zhang et al., 2007) and sensory neuron-specific Mas-related G protein-coupled receptors-X1 (MRGPR-X1) (Solinski et al., 2012). TRPV1 channels are inhibited by PIP_2 and PLCβ-mediated degradation of PIP_2 relieves TRPV1 from the inhibitory effects of PIP_2, thereby activating the ion channels (Chuang et al., 2001; Prescott and Julius, 2003; Suh and Hille, 2008). Consistent with this scenario, application of oxytocin, which differs from AVP in only two amino acids, activates TRPV1 channels in the subiculum via PIP_2 degradation (Hu et al., 2020a), and TRPV2 channels in the hypothalamic neurons via phosphoinositide 3-kinase (van den Burg et al., 2015). Because phosphoinositide 3-kinase converts PIP_2 to phosphatidylinositol-3, 4, 5-triphosphate (PIP_3), and PIP_2 interacts with a group of positive residues downstream the TRPbox of TRPV1 and TRPV2 (Taberner et al., 2015; Ufret-Vincenty et al., 2011), it is plausible that PIP_2 depletion catalyzed by phosphoinositide 3-kinase could be involved in oxytocin receptor-mediated facilitation of TRPV2 channels as well.

Our results also indicate that AVP excites about 40% subicular pyramidal neurons majorly via inhibition of Kir channels because the I-V curves of the AVP-elicited currents displayed the characteristics of Kir channels and application of Ba^{2+} at 300 μM significantly reduced AVP-induced inward currents. Consistent with our results, AVP has been shown to suppress Kir channels in porcine cerebral capillary endothelial cells (Hoyer et al., 1991). Furthermore, activation of oxytocin receptors inhibits Kir channels in the immortalized gonadotropin-releasing hormone-positive GN11 cell line (Gravati et al., 2010), the lateral nucleus of central amygdala neurons (Hu et al., 2020b) and subicular pyramidal neurons (Hu et al., 2020a). There are many subtypes of Kir channels and K_{ATP} channels are one of them. Whilst activation of V_{1a} receptors has been shown to depress K_{ATP} channels (Shi et al., 2007; Wakatsuki et al., 1992), it is unlikely that K_{ATP} channels are responsible for AVP-elicited excitation of subicular pyramidal neurons because our recording pipettes contained 2 mM ATP which inhibited K_{ATP} channels. Application of ML 133, the selective inhibitor for Kir2 subfamily (Ford and Baccei, 2016; Huang et al., 2018; Kim et al., 2015; Sonkusare et al., 2016; Wang et al., 2011) by itself failed to consistently and significantly elicit an inward current, although Kir2 channels are tonically active (Hibino et al., 2010). This may be due to the scarce expression of Kir2 subfamily in the subiculum (Karschin et al., 1996). Consistently, application of AVP still elicited a comparable inward current in the continuous presence of ML 133, demonstrating that V_{1a} receptor-elicited excitation of subicular pyramidal neurons is not mediated by depressing Kir2 subfamily. Our results indicate that GIRK channels are the subfamily involved in AVP-mediated excitation of subicular pyramidal neurons because application of SCH23390, the selective GIRK channel blocker, significantly reduced AVP-induced inward currents. If activation of V_{1a} receptors excites subicular pyramidal neurons by depression of GIRK channels, GIRK channels must be constitutively active. Consistent with this prerequisite, GIRK channels are constitutively

active (Chen and Johnston, 2005; Gonzalez et al., 2018). In line with this scenario, our results demonstrate that application of SCH23390 alone induced in inward current, suggesting that GIRK channels in the subicular pyramidal neurons are tonically active. GIRK channels contain 4 subunits including GIRK1, GIRK2, GIRK3 and GIRK4 and exist as predominantly heterotetramers of GIRK1, GIRK2 and/or GIRK3, or as homotetramers of the GIRK2 subunit (Hibino et al., 2010; Luscher and Slesinger, 2010). GIRK4 is restrictedly expressed in certain neuronal populations, such as Purkinje cells and neurons of the globus pallidus and the ventral pallidum (Murer et al., 1997). In the subiculum, the major GIRK subunits are GIRK1, GIRK2 and GIRK3 (Karschin et al., 1996) with much less expression of GIRK4 (Karschin et al., 1996; Spauschus et al., 1996). Whilst the GIRK subunits involved in V_{1a} receptor-elicited excitation of subicular pyramidal neurons remain to be determined, GIRK1 seems to be a candidate because we have shown that application of the selective GIRK1 activator, ML 297 (Kaufmann et al., 2013), induced an outward current. Consistent with our results, another neuropeptide, gastrin-releasing peptide excites rat paraventricular thalamic neurons by simultaneous suppression of Kir channels and activation of TRPV1 channels (Hermes et al., 2013), although the subtype of the Kir channels is Kir2 subfamily not GIRK channels as we demonstrated in the present study. Congruously, AVP excites motoneurons by activating a nonselective cationic conductance and suppressing a K^+ conductance (Kolaj and Renaud, 1998; Ogier et al., 2006; Raggenbass, 2008), although the identities of the cationic and K^+ channels have not been determined. Our study identified that the cationic and K^+ channels underlying V_{1a} receptor-mediated excitation of subicular pyramidal neurons are TRPV1 and GIRK channels, respectively.

How does V_{1a} receptor activation lead to depression of GIRK channels? Our results further demonstrate that PKC is required for AVP-mediated depression of GIRK channels in subicular pyramidal neurons. Consistent with our results, GIRK channels are inhibited by PKC-mediated phosphorylation (Adney et al., 2015; Mao et al., 2004; Stevens et al., 1999) and PKC-elicited suppression of GIRK channels is responsible for oxytocin receptor-mediated excitation of the lateral nucleus of central amygdala neurons (Hu et al., 2020b) and subicular pyramidal neurons (Hu et al., 2020a) as well.

The subiculum is the major output pathway of hippocampus and targets a variety of cortical areas and subcortical structures (O'Mara et al., 2001). This divergent output makes subiculum an integral component in networks underlying diverse functions and behaviors, such as regulation of spatial memory (O'Mara et al., 2001; O'Mara et al., 2009), the functions of hypothalamic-pituitary axis (O'Mara, 2005) and stress responses (Mueller et al., 2004). Additionally, dysregulation of subicular function has been implicated in pathological conditions such as epilepsy (Stafstrom, 2005; Wozny et al., 2005) and drug addiction (O'Mara et al., 2009). Vasopressinergic fibers project from the parvocellular neurons of the hypothalamus to discrete extrahypothalamic limbic brain regions including the hippocampus, subiculum, amygdala and nucleus accumbens (Buijs, 1978; Buijs and Swaab, 1979; DeVries et al., 1985; Hawthorn et al., 1985; Lang et al., 1983), although AVP immunoreactive cells have also been detected in many extrahypothalamic structures including the bed nucleus of stria terminalis, septal region, medial amygdala and locus coeruleus (Cilz et al., 2019). In the brain, AVP modulates a variety of physiological functions including emotional responses (Caldwell et al., 2008; Neumann and Landgraf,

2012), social behaviors (Cilz et al., 2019; Kompier et al., 2019), learning and memory (Caldwell et al., 2008; de Wied et al., 1993), nociception (Koshimizu and Tsujimoto, 2009) and circadian rhythms (Gizowski et al., 2017). Many of these functions are associated with the limbic structures including the subiculum. Because many structures in the limbic system are reciprocally connected, functional alteration of one component such as the subiculum would likely affect the general function of the limbic system. The cellular and molecular effects of AVP should contribute to its in vivo physiological functions. To date, at least two cellular and molecular mechanisms for AVP in the subiculum have been detected. First, bath application of AVP induced a long-term enhancement of EPSP amplitude recorded from subiculum neurons and the maximal effect could be observed 30–45 min after AVP application (Chepkova et al., 1995). Second, the current study suggested that activation of V_{1a} receptors exerted short-term (within 3–5 min) excitation of subicular pyramidal neurons. AVP-induced short- and long-term excitation of subiculum should contribute to its *in vivo* physiological functions such as learning and memory as well as emotional control. Whilst the cellular and molecular mechanisms underlying AVP-induced long-term facilitation of EPSP amplitudes in the subiculum have not been determined (Chepkova et al., 1995), our results demonstrate that activation of V_{1a} receptors excites subicular pyramidal neurons via PLCβ-, PKC- and PIP_2-mediated depression of GIRK channels and activation of TRPV1 channels. Knowing the molecular targets of V_{1a} receptors in the brain would shed light on understanding the functions of AVP *in vivo*. For example, activation of V_{1a} receptors exerts anxiogenic effects (Bielsky et al., 2005; Bielsky et al., 2004; Egashira et al., 2007; Landgraf et al., 1995; Simon et al., 2008), although the underlying cellular and molecular mechanisms have not been determined. Because TRPV1 channels (Ho et al., 2012; Marsch et al., 2007), GIRK channels (Pravetoni and Wickman, 2008; Victoria et al., 2016; Wydeven et al., 2014), PLCβ (McOmish et al., 2008; Xiao et al., 2012) and PKC (Bowers et al., 2000; Lesscher et al., 2008; Liu et al., 2014) are involved in the modulation of anxiety, our results may provide an ionic and signaling mechanisms to explain the anxiogenic effects of AVP. Furthermore, activation of V_{1a} receptors facilitates learning and memory (Bielsky et al., 2005; Nephew and Bridges, 2008) and both TRPV1 (Bannazadeh et al., 2017; Bashiri et al., 2018; Edwards, 2014; Genro et al., 2012) and GIRK channels (Mayfield et al., 2015) are involved in cognitive functions. Our results may therefore provide one of the cellular and molecular mechanisms to explain the effects of AVP on memory as well.

5. Conclusion

Whereas the subiculum receives vasopressinergic innervation and expresses vasopressin receptors, the effects of AVP in the subiculum and the underlying cellular and molecular mechanisms have not been determined. We demonstrate that activation of V_{1a} receptors excites subicular pyramidal neurons via activation of TRPV1 channels and depression of GIRK channels. V_{1a} receptor-elicited excitation requires the function of PLCβ but is independent of intracellular Ca^{2+} release. PKC is responsible for V_{1a} receptor-mediated depression of GIRK channels whereas PIP_2 depletion is involved in V_{1a} receptor-elicited activation of TRPV1 channels. Our results may provide one of the cellular and molecular mechanisms to explain the physiological functions of AVP *in vivo*.

Acknowledgments

This work was supported by the National Institute Of General Medical Sciences (NIGMS) and National Institute Of Mental Health (NIMH) grant R01MH118258 to S.L.

References

Adney SK, Ha J, Meng XY, Kawano T, Logothetis DE, 2015. A Critical Gating Switch at a Modulatory Site in Neuronal Kir3 Channels. J Neurosci 35, 14397–14405. [PubMed: 26490875]

Amadesi S, Nie J, Vergnolle N, Cottrell GS, Grady EF, Trevisani M, Manni C, Geppetti P, McRoberts JA, Ennes H, Davis JB, Mayer EA, Bunnett NW, 2004. Protease-activated receptor 2 sensitizes the capsaicin receptor transient receptor potential vanilloid receptor 1 to induce hyperalgesia. J Neurosci 24, 4300–4312. [PubMed: 15128844]

Bannazadeh M, Fatehi F, Fatemi I, Roohbakhsh A, Allahtavakoli M, Nasiri M, Azin M, Shamsizadeh A, 2017. The role of transient receptor potential vanilloid type 1 in unimodal and multimodal object recognition task in rats. Pharmacol Rep 69, 526–531.

Bashiri H, Hosseini-Chegeni H, Alsadat Sharifi K, Sahebgharani M, Salari AA, 2018. Activation of TRPV1 receptors affects memory function and hippocampal TRPV1 and CREB mRNA expression in a rat model of biliary cirrhosis. Neurol Res 40, 938–947. [PubMed: 30079821]

Bielsky IF, Hu SB, Ren X, Terwilliger EF, Young LJ, 2005. The V1a vasopressin receptor is necessary and sufficient for normal social recognition: a gene replacement study. Neuron 47, 503–513. [PubMed: 16102534]

Bielsky IF, Hu SB, Szegda KL, Westphal H, Young LJ, 2004. Profound impairment in social recognition and reduction in anxiety-like behavior in vasopressin V1a receptor knockout mice. Neuropsychopharmacology 29, 483–493. [PubMed: 14647484]

Bowers BJ, Collins AC, Tritto T, Wehner JM, 2000. Mice lacking PKC gamma exhibit decreased anxiety. Behav Genet 30, 111–121. [PubMed: 10979601]

Buijs RM, 1978. Intra- and extrahypothalamic vasopressin and oxytocin pathways in the rat. Pathways to the limbic system, medulla oblongata and spinal cord. Cell Tissue Res 192, 423–435. [PubMed: 699026]

Buijs RM, Swaab DF, 1979. Immuno-electron microscopical demonstration of vasopressin and oxytocin synapses in the limbic system of the rat. Cell Tissue Res 204, 355–365. [PubMed: 527026]

Caffe AR, van Leeuwen FW, 1983. Vasopressin-immunoreactive cells in the dorsomedial hypothalamic region, medial amygdaloid nucleus and locus coeruleus of the rat. Cell Tissue Res 233, 23–33. [PubMed: 6616564]

Caldwell HK, Lee HJ, Macbeth AH, Young WS 3rd, 2008. Vasopressin: behavioral roles of an “original” neuropeptide. Prog Neurobiol 84, 1–24. [PubMed: 18053631]

Chee MJ, Price CJ, Statnick MA, Colmers WF, 2011. Nociceptin/orphanin FQ suppresses the excitability of neurons in the ventromedial nucleus of the hypothalamus. J Physiol 589, 3103–3114. [PubMed: 21502286]

Chen X, Johnston D, 2005. Constitutively active G-protein-gated inwardly rectifying K+ channels in dendrites of hippocampal CA1 pyramidal neurons. J Neurosci 25, 3787–3792. [PubMed: 15829630]

Chepkova AN, French P, De Wied D, Ontskul AH, Ramakers GM, Skrebitski VG, Gispen WH, Urban IJ, 1995. Long-lasting enhancement of synaptic excitability of CA1/subiculum neurons of the rat ventral hippocampus by vasopressin and vasopressin(4–8). Brain Res 701, 255–266. [PubMed: 8925289]

Chuang HH, Prescott ED, Kong H, Shields S, Jordt SE, Basbaum AI, Chao MV, Julius D, 2001. Bradykinin and nerve growth factor release the capsaicin receptor from PtdIns(4,5)P2-mediated inhibition. Nature 411, 957–962. [PubMed: 11418861]

Cilz NI, Cymerblit-Sabba A, Young WS, 2019. Oxytocin and vasopressin in the rodent hippocampus. Genes Brain Behav 18, e12535. [PubMed: 30378258]

de Wied D, Diamant M, Fodor M, 1993. Central nervous system effects of the neurohypophyseal hormones and related peptides. Front Neuroendocrinol 14, 251–302. [PubMed: 8258377]

DeVries GJ, Buijs RM, Van Leeuwen FW, Caffe AR, Swaab DF, 1985. The vasopressinergic innervation of the brain in normal and castrated rats. J Comp Neurol 233, 236–254. [PubMed: 3882778]

Edwards JG, 2014. TRPV1 in the central nervous system: synaptic plasticity, function, and pharmacological implications. Prog Drug Res 68, 77–104. [PubMed: 24941665]

Egashira N, Tanoue A, Matsuda T, Koushi E, Harada S, Takano Y, Tsujimoto G, Mishima K, Iwasaki K, Fujiwara M, 2007. Impaired social interaction and reduced anxiety-related behavior in vasopressin V1a receptor knockout mice. Behav Brain Res 178, 123–127. [PubMed: 17227684]

Ford NC, Baccei ML, 2016. Inward-rectifying K(+) (Kir2) leak conductance dampens the excitability of lamina I projection neurons in the neonatal rat. Neuroscience 339, 502–510. [PubMed: 27751963]

Genro BP, de Oliveira Alvares L, Quillfeldt JA, 2012. Role of TRPV1 in consolidation of fear memories depends on the averseness of the conditioning procedure. Neurobiol Learn Mem 97, 355–360. [PubMed: 22270459]

Gizowski C, Trudel E, Bourque CW, 2017. Central and peripheral roles of vasopressin in the circadian defense of body hydration. Best Pract Res Clin Endocrinol Metab 31, 535–546. [PubMed: 29224666]

Gonzalez JC, Epps SA, Markwardt SJ, Wadiche JI, Overstreet-Wadiche L, 2018. Constitutive and Synaptic Activation of GIRK Channels Differentiates Mature and Newborn Dentate Granule Cells. J Neurosci 38, 6513–6526. [PubMed: 29915136]

Gravati M, Busnelli M, Bulgheroni E, Reversi A, Spaiardi P, Parenti M, Toselli M, Chini B, 2010. Dual modulation of inward rectifier potassium currents in olfactory neuronal cells by promiscuous G protein coupling of the oxytocin receptor. J Neurochem 114, 1424–1435. [PubMed: 20557424]

Graves AR, Moore SJ, Bloss EB, Mensh BD, Kath WL, Spruston N, 2012. Hippocampal pyramidal neurons comprise two distinct cell types that are countermodulated by metabotropic receptors. Neuron 76, 776–789. [PubMed: 23177962]

Hawthorn J, Ang VT, Jenkins JS, 1985. Effects of lesions in the hypothalamic paraventricular, supraoptic and suprachiasmatic nuclei on vasopressin and oxytocin in rat brain and spinal cord. Brain Res 346, 51–57. [PubMed: 4052770]

Hermes ML, Kolaj M, Coderre EM, Renaud LP, 2013. Gastrin-releasing peptide acts via postsynaptic BB2 receptors to modulate inward rectifier K+ and TRPV1-like conductances in rat paraventricular thalamic neurons. J Physiol 591, 1823–1839. [PubMed: 23359674]

Hibino H, Inanobe A, Furutani K, Murakami S, Findlay I, Kurachi Y, 2010. Inwardly rectifying potassium channels: their structure, function, and physiological roles. Physiol Rev 90, 291–366. [PubMed: 20086079]

Ho KW, Ward NJ, Calkins DJ, 2012. TRPV1: a stress response protein in the central nervous system. Am J Neurodegener Dis 1, 1–14. [PubMed: 22737633]

Hoyer J, Popp R, Meyer J, Galla HJ, Gogelein H, 1991. Angiotensin II, vasopressin and GTP[gamma-S] inhibit inward-rectifying K+ channels in porcine cerebral capillary endothelial cells. J Membr Biol 123, 55–62. [PubMed: 1774774]

Hu B, Boyle CA, Lei S, 2020a. Activation of Oxytocin Receptors Excites Subicular Neurons by Multiple Signaling and Ionic Mechanisms. Cereb Cortex.

Hu B, Boyle CA, Lei S, 2020b. Oxytocin receptors excite lateral nucleus of central amygdala by phospholipase Cbeta- and protein kinase C-dependent depression of inwardly rectifying K(+) channels. J Physiol 598, 3501–3520. [PubMed: 32458437]

Hu B, Cilz NI, Lei S, 2017. Somatostatin depresses the excitability of subicular bursting cells: Roles of inward rectifier K(+) channels, KCNQ channels and Epac. Hippocampus 27, 971–984. [PubMed: 28558129]

Huang X, Lee SH, Lu H, Sanders KM, Koh SD, 2018. Molecular and functional characterization of inwardly rectifying K(+) currents in murine proximal colon. J Physiol 596, 379–391. [PubMed: 29205356]

Insel TR, Wang ZX, Ferris CF, 1994. Patterns of brain vasopressin receptor distribution associated with social organization in microtine rodents. J Neurosci 14, 5381–5392. [PubMed: 8083743]

Joksimovic SM, Eggan P, Izumi Y, Joksimovic SL, Tesic V, Dietz RM, Orfila JE, DiGruccio MR, Herson PS, Jevtovic-Todorovic V, Zorumski CF, Todorovic SM, 2017. The role of T-type calcium channels in the subiculum: to burst or not to burst? J Physiol 595, 6327–6348. [PubMed: 28744923]

Karschin C, Dissmann E, Stuhmer W, Karschin A, 1996. IRK(1–3) and GIRK(1–4) inwardly rectifying K+ channel mRNAs are differentially expressed in the adult rat brain. J Neurosci 16, 3559–3570. [PubMed: 8642402]

Kaufmann K, Romaine I, Days E, Pascual C, Malik A, Yang L, Zou B, Du Y, Sliwoski G, Morrison RD, Denton J, Niswender CM, Daniels JS, Sulikowski GA, Xie XS, Lindsley CW, Weaver CD, 2013. ML297 (VU0456810), the first potent and selective activator of the GIRK potassium channel, displays antiepileptic properties in mice. ACS Chem Neurosci 4, 1278–1286. [PubMed: 23730969]

Kim KS, Jang JH, Lin H, Choi SW, Kim HR, Shin DH, Nam JH, Zhang YH, Kim SJ, 2015. Rise and Fall of Kir2.2 Current by TLR4 Signaling in Human Monocytes: PKC-Dependent Trafficking and PI3K-Mediated PIP2 Decrease. J Immunol 195, 3345–3354. [PubMed: 26324774]

Kolaj M, Renaud LP, 1998. Vasopressin-induced currents in rat neonatal spinal lateral horn neurons are G-protein mediated and involve two conductances. J Neurophysiol 80, 1900–1910. [PubMed: 9772248]

Kompier NF, Keysers C, Gazzola V, Lucassen PJ, Krugers HJ, 2019. Early Life Adversity and Adult Social Behavior: Focus on Arginine Vasopressin and Oxytocin as Potential Mediators. Front Behav Neurosci 13, 143. [PubMed: 31404254]

Koshimizu TA, Tsujimoto G, 2009. New topics in vasopressin receptors and approach to novel drugs: vasopressin and pain perception. J Pharmacol Sci 109, 33–37. [PubMed: 19151539]

Kuzhikandathil EV, Oxford GS, 2002. Classic D1 dopamine receptor antagonist R-(+)-7-chloro-8-hydroxy-3-methyl-1-phenyl-2,3,4,5-tetrahydro-1H-3-benzazepine hydrochloride (SCH23390) directly inhibits G protein-coupled inwardly rectifying potassium channels. Mol Pharmacol 62, 119–126. [PubMed: 12065762]

Lacey MG, Mercuri NB, North RA, 1988. On the potassium conductance increase activated by GABAB and dopamine D2 receptors in rat substantia nigra neurones. J Physiol 401, 437–453. [PubMed: 2459376]

Landgraf R, Gerstberger R, Montkowski A, Probst JC, Wotjak CT, Holsboer F, Engelmann M, 1995. V1 vasopressin receptor antisense oligodeoxynucleotide into septum reduces vasopressin binding, social discrimination abilities, and anxiety-related behavior in rats. J Neurosci 15, 4250–4258. [PubMed: 7790909]

Lang RE, Heil J, Ganten D, Hermann K, Rascher W, Unger T, 1983. Effects of lesions in the paraventricular nucleus of the hypothalamus on vasopressin and oxytocin contents in brainstem and spinal cord of rat. Brain Res 260, 326–329. [PubMed: 6831205]

Lesscher HM, McMahon T, Lasek AW, Chou WH, Connolly J, Kharazia V, Messing RO, 2008. Amygdala protein kinase C epsilon regulates corticotropin-releasing factor and anxiety-like behavior. Genes Brain Behav 7, 323–333. [PubMed: 17908177]

Li H, Hu B, Zhang HP, Boyle CA, Lei S, 2019. Roles of K(+) and cation channels in ORL-1 receptor-mediated depression of neuronal excitability and epileptic activities in the medial entorhinal cortex. Neuropharmacology 151, 144–158. [PubMed: 30998945]

Liu B, Feng J, Wang JH, 2014. Protein kinase C is essential for kainate-induced anxiety-related behavior and glutamatergic synapse upregulation in prelimbic cortex. CNS Neurosci Ther 20, 982–990. [PubMed: 25180671]

Luscher C, Slesinger PA, 2010. Emerging roles for G protein-gated inwardly rectifying potassium (GIRK) channels in health and disease. Nat Rev Neurosci 11, 301–315. [PubMed: 20389305]

Mao J, Wang X, Chen F, Wang R, Rojas A, Shi Y, Piao H, Jiang C, 2004. Molecular basis for the inhibition of G protein-coupled inward rectifier K(+) channels by protein kinase C. Proc Natl Acad Sci U S A 101, 1087–1092. [PubMed: 14732702]

Marsch R, Foeller E, Rammes G, Bunck M, Kossl M, Holsboer F, Zieglgansberger W, Landgraf R, Lutz B, Wotjak CT, 2007. Reduced anxiety, conditioned fear, and hippocampal long-term

potentiation in transient receptor potential vanilloid type 1 receptor-deficient mice. J Neurosci 27, 832–839. [PubMed: 17251423]

Mason A, 1993. Electrophysiology and burst-firing of rat subicular pyramidal neurons in vitro: a comparison with area CA1. Brain Res 600, 174–178. [PubMed: 8422585]

Mattia D, Hwa GG, Avoli M, 1993. Membrane properties of rat subicular neurons in vitro. J Neurophysiol 70, 1244–1248. [PubMed: 8229171]

Mayfield J, Blednov YA, Harris RA, 2015. Behavioral and Genetic Evidence for GIRK Channels in the CNS: Role in Physiology, Pathophysiology, and Drug Addiction. Int Rev Neurobiol 123, 279–313. [PubMed: 26422988]

McOmish CE, Burrows EL, Howard M, Hannan AJ, 2008. PLC-beta1 knockout mice as a model of disrupted cortical development and plasticity: behavioral endophenotypes and dysregulation of RGS4 gene expression. Hippocampus 18, 824–834. [PubMed: 18493969]

Moriyama T, Higashi T, Togashi K, Iida T, Segi E, Sugimoto Y, Tominaga T, Narumiya S, Tominaga M, 2005. Sensitization of TRPV1 by EP1 and IP reveals peripheral nociceptive mechanism of prostaglandins. Mol Pain 1, 3. [PubMed: 15813989]

Mueller NK, Dolgas CM, Herman JP, 2004. Stressor-selective role of the ventral subiculum in regulation of neuroendocrine stress responses. Endocrinology 145, 3763–3768. [PubMed: 15142982]

Murer G, Adelbrecht C, Lauritzen I, Lesage F, Lazdunski M, Agid Y, Raisman-Vozari R, 1997. An immunocytochemical study on the distribution of two G-protein-gated inward rectifier potassium channels (GIRK2 and GIRK4) in the adult rat brain. Neuroscience 80, 345–357. [PubMed: 9284339]

Nephew BC, Bridges RS, 2008. Arginine vasopressin V1a receptor antagonist impairs maternal memory in rats. Physiol Behav 95, 182–186. [PubMed: 18620713]

Neumann ID, Landgraf R, 2012. Balance of brain oxytocin and vasopressin: implications for anxiety, depression, and social behaviors. Trends Neurosci 35, 649–659. [PubMed: 22974560]

O'Mara S, 2005. The subiculum: what it does, what it might do, and what neuroanatomy has yet to tell us. J Anat 207, 271–282. [PubMed: 16185252]

O'Mara SM, Commins S, Anderson M, Gigg J, 2001. The subiculum: a review of form, physiology and function. Prog Neurobiol 64, 129–155. [PubMed: 11240210]

O'Mara SM, Sanchez-Vives MV, Brotons-Mas JR, O'Hare E, 2009. Roles for the subiculum in spatial information processing, memory, motivation and the temporal control of behaviour. Prog Neuropsychopharmacol Biol Psychiatry 33, 782–790. [PubMed: 19393282]

Ogier R, Tribollet E, Suarez P, Raggenbass M, 2006. Identified motoneurons involved in sexual and eliminative functions in the rat are powerfully excited by vasopressin and tachykinins. J Neurosci 26, 10717–10726. [PubMed: 17050711]

Otero-Garcia M, Agustin-Pavon C, Lanuza E, Martinez-Garcia F, 2016. Distribution of oxytocin and co-localization with arginine vasopressin in the brain of mice. Brain Struct Funct 221, 3445–3473. [PubMed: 26388166]

Phillips PA, Abrahams JM, Kelly J, Paxinos G, Grzonka Z, Mendelsohn FA, Johnston CI, 1988. Localization of vasopressin binding sites in rat brain by in vitro autoradiography using a radioiodinated V1 receptor antagonist. Neuroscience 27, 749–761. [PubMed: 3252172]

Plant TD, Zollner C, Kepura F, Mousa SS, Eichhorst J, Schaefer M, Furkert J, Stein C, Oksche A, 2007. Endothelin potentiates TRPV1 via ETA receptor-mediated activation of protein kinase C. Mol Pain 3, 35. [PubMed: 18001466]

Pravetoni M, Wickman K, 2008. Behavioral characterization of mice lacking GIRK/Kir3 channel subunits. Genes Brain Behav 7, 523–531. [PubMed: 18194467]

Prescott ED, Julius D, 2003. A modular PIP2 binding site as a determinant of capsaicin receptor sensitivity. Science 300, 1284–1288. [PubMed: 12764195]

Raggenbass M, 2008. Overview of cellular electrophysiological actions of vasopressin. Eur J Pharmacol 583, 243–254. [PubMed: 18280467]

Ramanathan G, Cilz NI, Kurada L, Hu B, Wang X, Lei S, 2012. Vasopressin facilitates GABAergic transmission in rat hippocampus via activation of V(1A) receptors. Neuropharmacology 63, 1218–1226. [PubMed: 22884625]

Rodriguez-Menchaca AA, Adney SK, Zhou L, Logothetis DE, 2012. Dual Regulation of Voltage-Sensitive Ion Channels by PIP(2). Front Pharmacol 3, 170. [PubMed: 23055973]

Sculptoreanu A, Aura Kullmann F, de Groat WC, 2008. Neurokinin 2 receptor-mediated activation of protein kinase C modulates capsaicin responses in DRG neurons from adult rats. Eur J Neurosci 27, 3171–3181. [PubMed: 18598261]

Shi W, Cui N, Shi Y, Zhang X, Yang Y, Jiang C, 2007. Arginine vasopressin inhibits Kir6.1/SUR2B channel and constricts the mesenteric artery via V1a receptor and protein kinase C. Am J Physiol Regul Integr Comp Physiol 293, R191–199. [PubMed: 17428891]

Shim WS, Tak MH, Lee MH, Kim M, Kim M, Koo JY, Lee CH, Kim M, Oh U, 2007. TRPV1 mediates histamine-induced itching via the activation of phospholipase A2 and 12-lipoxygenase. J Neurosci 27, 2331–2337. [PubMed: 17329430]

Shin J, Cho H, Hwang SW, Jung J, Shin CY, Lee SY, Kim SH, Lee MG, Choi YH, Kim J, Haber NA, Reichling DB, Khasar S, Levine JD, Oh U, 2002. Bradykinin-12-lipoxygenase-VR1 signaling pathway for inflammatory hyperalgesia. Proc Natl Acad Sci U S A 99, 10150–10155. [PubMed: 12097645]

Simon NG, Guillon C, Fabio K, Heindel ND, Lu SF, Miller M, Ferris CF, Brownstein MJ, Garripa C, Koppel GA, 2008. Vasopressin antagonists as anxiolytics and antidepressants: recent developments. Recent Pat CNS Drug Discov 3, 77–93. [PubMed: 18537767]

Sofroniew MV, 1985. Vasopressin- and neurophysin-immunoreactive neurons in the septal region, medial amygdala and locus coeruleus in colchicine-treated rats. Neuroscience 15, 347–358. [PubMed: 4022328]

Solinski HJ, Zierler S, Gudermann T, Breit A, 2012. Human sensory neuron-specific Mas-related G protein-coupled receptors-X1 sensitize and directly activate transient receptor potential cation channel V1 via distinct signaling pathways. J Biol Chem 287, 40956–40971. [PubMed: 23074220]

Sonkusare SK, Dalsgaard T, Bonev AD, Nelson MT, 2016. Inward rectifier potassium (Kir2.1) channels as end-stage boosters of endothelium-dependent vasodilators. J Physiol 594, 3271–3285. [PubMed: 26840527]

Spauschus A, Lentes KU, Wischmeyer E, Dissmann E, Karschin C, Karschin A, 1996. A G-protein-activated inwardly rectifying K+ channel (GIRK4) from human hippocampus associates with other GIRK channels. J Neurosci 16, 930–938. [PubMed: 8558261]

Stafstrom CE, 2005. The role of the subiculum in epilepsy and epileptogenesis. Epilepsy Curr 5, 121–129. [PubMed: 16151518]

Stevens EB, Shah BS, Pinnock RD, Lee K, 1999. Bombesin receptors inhibit G protein-coupled inwardly rectifying K+ channels expressed in Xenopus oocytes through a protein kinase C-dependent pathway. Mol Pharmacol 55, 1020–1027. [PubMed: 10347243]

Stoop R, 2012. Neuromodulation by oxytocin and vasopressin. Neuron 76, 142–159. [PubMed: 23040812]

Suh BC, Hille B, 2008. PIP2 is a necessary cofactor for ion channel function: how and why? Annu Rev Biophys 37, 175–195. [PubMed: 18573078]

Taberner FJ, Fernandez-Ballester G, Fernandez-Carvajal A, Ferrer-Montiel A, 2015. TRP channels interaction with lipids and its implications in disease. Biochim Biophys Acta 1848, 1818–1827. [PubMed: 25838124]

Ufret-Vincenty CA, Klein RM, Hua L, Angueyra J, Gordon SE, 2011. Localization of the PIP2 sensor of TRPV1 ion channels. J Biol Chem 286, 9688–9698. [PubMed: 21224382]

van den Burg EH, Stindl J, Grund T, Neumann ID, Strauss O, 2015. Oxytocin Stimulates Extracellular Ca2+ Influx Through TRPV2 Channels in Hypothalamic Neurons to Exert Its Anxiolytic Effects. Neuropsychopharmacology 40, 2938–2947. [PubMed: 26013963]

van Leeuwen F, Caffe R, 1983. Vasopressin-immunoreactive cell bodies in the bed nucleus of the stria terminalis of the rat. Cell Tissue Res 228, 525–534. [PubMed: 6339062]

Victoria NC, Marron Fernandez de Velasco E, Ostrovskaya O, Metzger S, Xia Z, Kotecki L, Benneyworth MA, Zink AN, Martemyanov KA, Wickman K, 2016. G Protein-Gated K(+) Channel Ablation in Forebrain Pyramidal Neurons Selectively Impairs Fear Learning. Biol Psychiatry 80, 796–806. [PubMed: 26612516]

Wakatsuki T, Nakaya Y, Inoue I, 1992. Vasopressin modulates K(+)-channel activities of cultured smooth muscle cells from porcine coronary artery. Am J Physiol 263, H491–496. [PubMed: 1387293]

Wang HR, Wu M, Yu H, Long S, Stevens A, Engers DW, Sackin H, Daniels JS, Dawson ES, Hopkins CR, Lindsley CW, Li M, McManus OB, 2011. Selective inhibition of the K(ir)2 family of inward rectifier potassium channels by a small molecule probe: the discovery, SAR, and pharmacological characterization of ML133. ACS Chem Biol 6, 845–856. [PubMed: 21615117]

Wozny C, Knopp A, Lehmann TN, Heinemann U, Behr J, 2005. The subiculum: a potential site of ictogenesis in human temporal lobe epilepsy. Epilepsia 46 Suppl 5, 17–21.

Wozny C, Maier N, Schmitz D, Behr J, 2008. Two different forms of long-term potentiation at CA1-subiculum synapses. J Physiol 586, 2725–2734. [PubMed: 18403426]

Wu LJ, Sweet TB, Clapham DE, 2010. International Union of Basic and Clinical Pharmacology. LXXVI. Current progress in the mammalian TRP ion channel family. Pharmacol Rev 62, 381–404. [PubMed: 20716668]

Wydeven N, Marron Fernandez de Velasco E, Du Y, Benneyworth MA, Hearing MC, Fischer RA, Thomas MJ, Weaver CD, Wickman K, 2014. Mechanisms underlying the activation of G-protein-gated inwardly rectifying K+ (GIRK) channels by the novel anxiolytic drug, ML297. Proc Natl Acad Sci U S A 111, 10755–10760. [PubMed: 25002517]

Xiao Z, Jaiswal MK, Deng PY, Matsui T, Shin HS, Porter JE, Lei S, 2012. Requirement of phospholipase C and protein kinase C in cholecystokinin-mediated facilitation of NMDA channel function and anxiety-like behavior. Hippocampus 22, 1438–1450. [PubMed: 22072552]

Zhang H, Cang CL, Kawasaki Y, Liang LL, Zhang YQ, Ji RR, Zhao ZQ, 2007. Neurokinin-1 receptor enhances TRPV1 activity in primary sensory neurons via PKCepsilon: a novel pathway for heat hyperalgesia. J Neurosci 27, 12067–12077. [PubMed: 17978048]

Highlights

- Activation of V_{1a} receptors excites subicular pyramidal neurons
- V_{1a} receptor-induced excitation is mediated primarily by activation of TRPV1 channels in ~60% subicular pyramidal neurons
- Inhibition of GIRK channels is responsible for V_{1a} receptor-elicited excitation in ~40% subicular pyramidal neurons
- PLCβ not intracellular Ca^{2+} is necessary for V_{1a} receptor-mediated excitation of subicular pyramidal neurons
- PKC is responsible for V_{1a} receptor-elicited inhibition of GIRK channels, whereas PIP_2 degradation is involved in V_{1a} receptor-mediated activation of TRPV1 channels

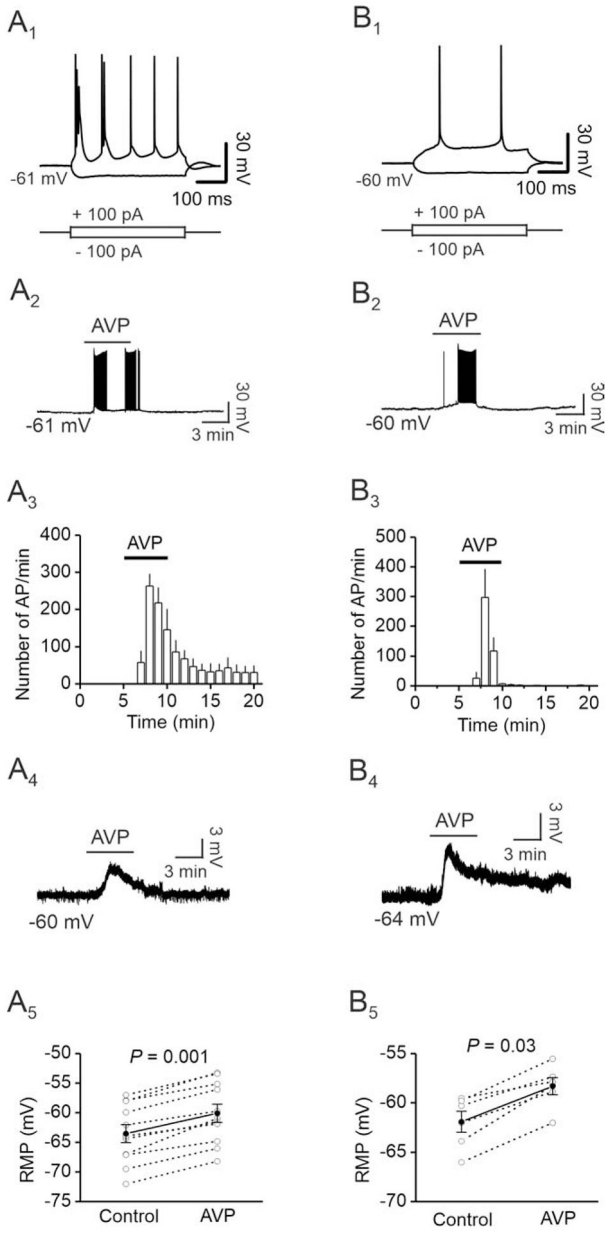

Figure 1. AVP excites both bursting cells and regular firing cells.

A_1-A_5, Bath application of AVP excited bursting cells by eliciting AP firing or subthreshold depolarization. **A_1**, Voltage responses (*Upper panel*) elicited by a negative (−100 pA) and a positive (+100 pA) current injection (*Lower panel*). Note the initial bursting response evoked by the positive current injection. **A_2**, Application of AVP elicited transient AP firing recorded from the RMP of the same neuron. **A_3**, Average of the AP numbers pooled from 17 bursting cells. **A_4**, Subthreshold depolarization evoked by AVP in a bursting cell. **A_5**, Summary graph showing subthreshold depolarization elicited by AVP in 11 bursting cells. **B_1-B_5**, Bath application of AVP excited regular firing cells by eliciting AP firing or subthreshold depolarization. **B_1**, Voltage responses (*Upper panel*) elicited by a negative (−100 pA) and a positive (+100 pA) current injection (*Lower panel*). Note the regular AP

firing evoked by the positive current injection. **B_2**, Application of AVP elicited transient AP firing recorded from the RMP of the same neuron. **B_3**, Average of the AP numbers pooled from 6 regular firing cells. **B_4**, Subthreshold depolarization evoked by AVP in a regular firing cell. **B_5**, Summary graph showing subthreshold depolarization elicited by AVP in 6 regular firing cells.

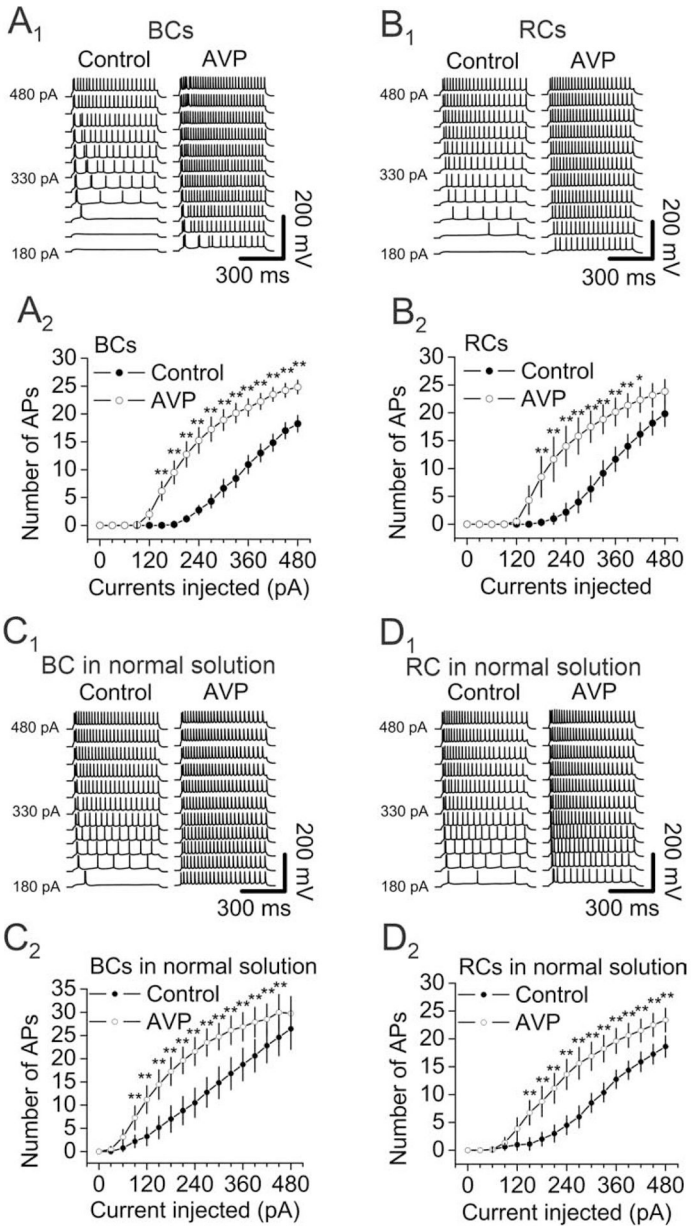

Figure 2. AVP increases the excitability of subicular pyramidal neurons evoked by injecting a series of positive currents.

A_1-A_2, Bath application of AVP increased the excitability of BCs evoked by injecting a series of positive currents from 30 pA to 480 pA at an interval of 30 pA and duration of 600 ms. The experiment was performed in the extracellular solution containing 1 mM kynurenic acid and 100 μM picrotoxin to block synaptic transmission. **A_1**, Current traces recorded from a BC before (*left*) and during (*right*) the application of AVP. **A_2**, Current-AP relationship constructed from 12 BCs before and during the application of AVP. ** $P < 0.01$. **B_1-B_2**, Bath application of AVP excited RCs elicited by injecting a series of positive currents from 30 pA to 480 pA at an interval of 30 pA and duration of 600 ms. The experiment was performed in the extracellular solution containing 1 mM kynurenic acid and 100 μM picrotoxin to block synaptic transmission. **B_1**, Current traces recorded from a RC before (*left*) and during (*right*)

the application of AVP. **B_2**, Current-AP relationship constructed from 6 RCs before and during the application of AVP. * $P < 0.05$, ** $P < 0.01$. **C_1-C_2**, Bath application of AVP increased the excitability of BCs evoked by the same current injection protocol in normal extracellular solution. **C_1**, Current traces recorded from a BC before (*left*) and during (*right*) the application of AVP in normal extracellular solution. **C_2**, Current-AP relationship constructed from 16 BCs before and during the application of AVP in normal extracellular solution. ** $P < 0.01$. **D_1-D_2**, Bath application of AVP excited RCs elicited by the positive current injection protocol in normal extracellular solution. **D_1**, Current traces recorded from a RC before (*left*) and during (*right*) the application of AVP in normal extracellular solution. **D_2**, Current-AP relationship constructed from 8 RCs before and during the application of AVP in normal extracellular solution. ** $P < 0.01$.

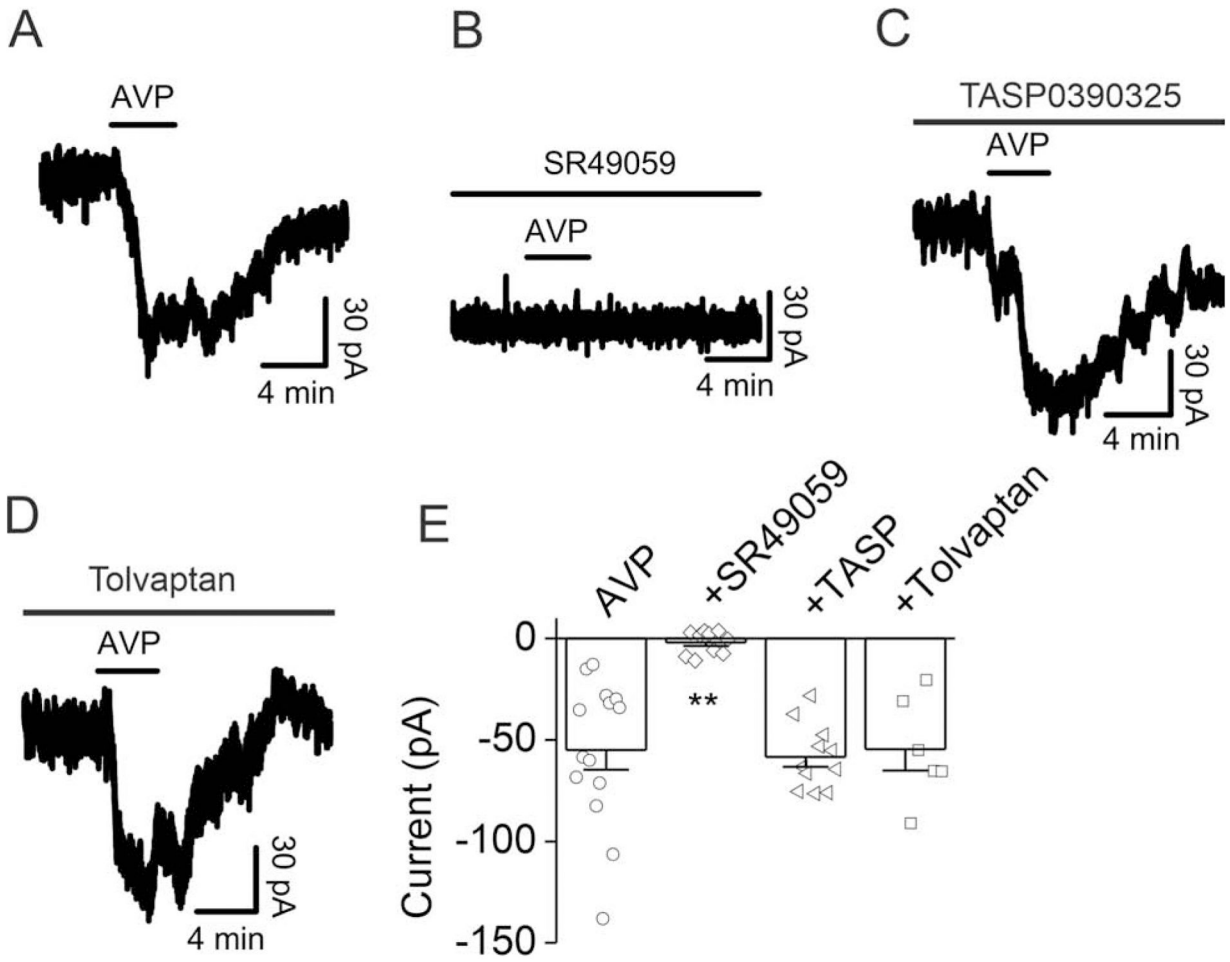

Figure 3. AVP excites subicular pyramidal neurons by activation of V_{1a} receptors.

A, Bath application of AVP generated an inward current recorded at −60 mV in a subicular pyramidal neuron. **B**, Pretreatment of slices with and continuous bath application of the selective V_{1a} receptor antagonist, SR49059 (1 μM), blocked AVP-elicited inward currents. **C**, Pretreatment of slices with and continuous bath application of the selective V_{1b} antagonist, TASP0390325 (TASP, 0.5 μM), had no effect on AVP-mediated inward currents. **D**, Pretreatment of slices with and continuous bath application of the selective V_2 antagonist, tolvaptan (50 nM), did not affect AVP-induced inward currents. **E**, Summary graph. Empty symbols represented values from individual cells and bar graphs were their averages. ** P <0.0001 vs. AVP alone.

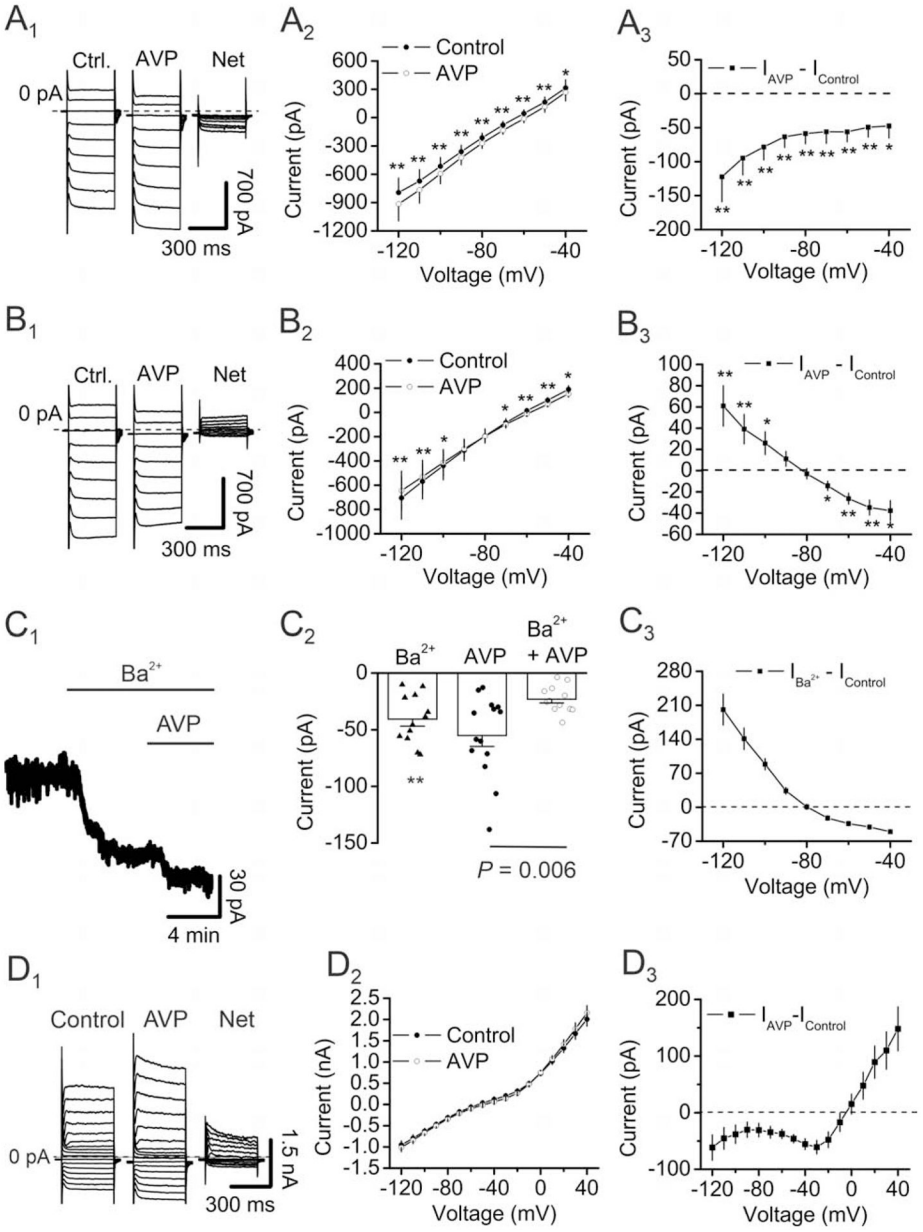

Figure 4. AVP excites subicular pyramidal neurons by activating a cationic channel and depressing a GIRK channel.

A_1-A_3: Application of AVP excited a subpopulation of subicular pyramidal neurons by activating a cationic conductance. **A_1**, Currents recorded from a subicular pyramidal neuron in response to the voltage-step protocol before (*left*) and during (*middle*) the application of AVP and the net current obtained by subtraction (*right*). The dash line was the zero current level. **A_2**, I-V curves of the currents elicited by the voltage-step protocol before and during the application of AVP (n = 12, * $P < 0.05$, ** $P < 0.01$). **A_3**, Net currents obtained by subtracting the currents in control condition from those recorded from the same cells during the application of AVP. **B_1-B_3**: Application of AVP excited a subpopulation of subicular pyramidal neurons by depressing Kir channels. **B_1**, Currents recorded from a subicular pyramidal neuron in response to the voltage-step protocol before (*left*) and during (*middle*)

the application of AVP and the net current obtained by subtraction (*right*). The dash line was the zero current level. **B_2**, I-V curves of the currents elicited by the voltage-step protocol before and during the application of AVP (n = 8, * $P < 0.05$, ** $P < 0.01$). **B_3**, Net currents obtained by subtracting the currents in control condition from those recorded from the same cells during the application of AVP. **C_1-C_3**, bath application of Ba^{2+} (300 μM) by itself inhibited Kir currents and significantly reduced AVP-elicited inward currents. **C_1**, Current trace recorded from a subicular pyramidal neuron in response to bath application of Ba^{2+} and Ba^{2+} plus AVP. **C_2**, Summary graph. Note that bath application of Ba^{2+} induced an inward current (** $P < 0.01$ vs. baseline) and significantly reduced AVP-elicited inward currents. **C_3**, I-V curve of the net currents elicited by Ba^{2+} (300 μM) showed inward rectification (n = 5). **D_1-D_3**, In the continuous presence of Ba^{2+} (300 μM), AVP elicited a cationic channel current with a reversal potential at about −15 mV. **D_1**, Current traces evoked by a voltage step protocol (from −120 mV to +40 mV for 400 ms at a voltage interval of 10 mV every 10 s) before (*left*) and during (*middle*) the application of AVP and the net current obtained by subtraction (*right*). The dash line was the zero current level. Steady-state currents were measured within 5 ms before the end of the step voltage protocols. **D_2**, I-V curves of the currents elicited by the voltage-step protocol before and during the application of AVP in the continuous presence of Ba^{2+} (n = 11). **D_3**, net currents obtained by subtracting the currents in the presence of Ba^{2+} alone from those recorded from the same cells in the presence of both Ba^{2+} and AVP (n = 11).

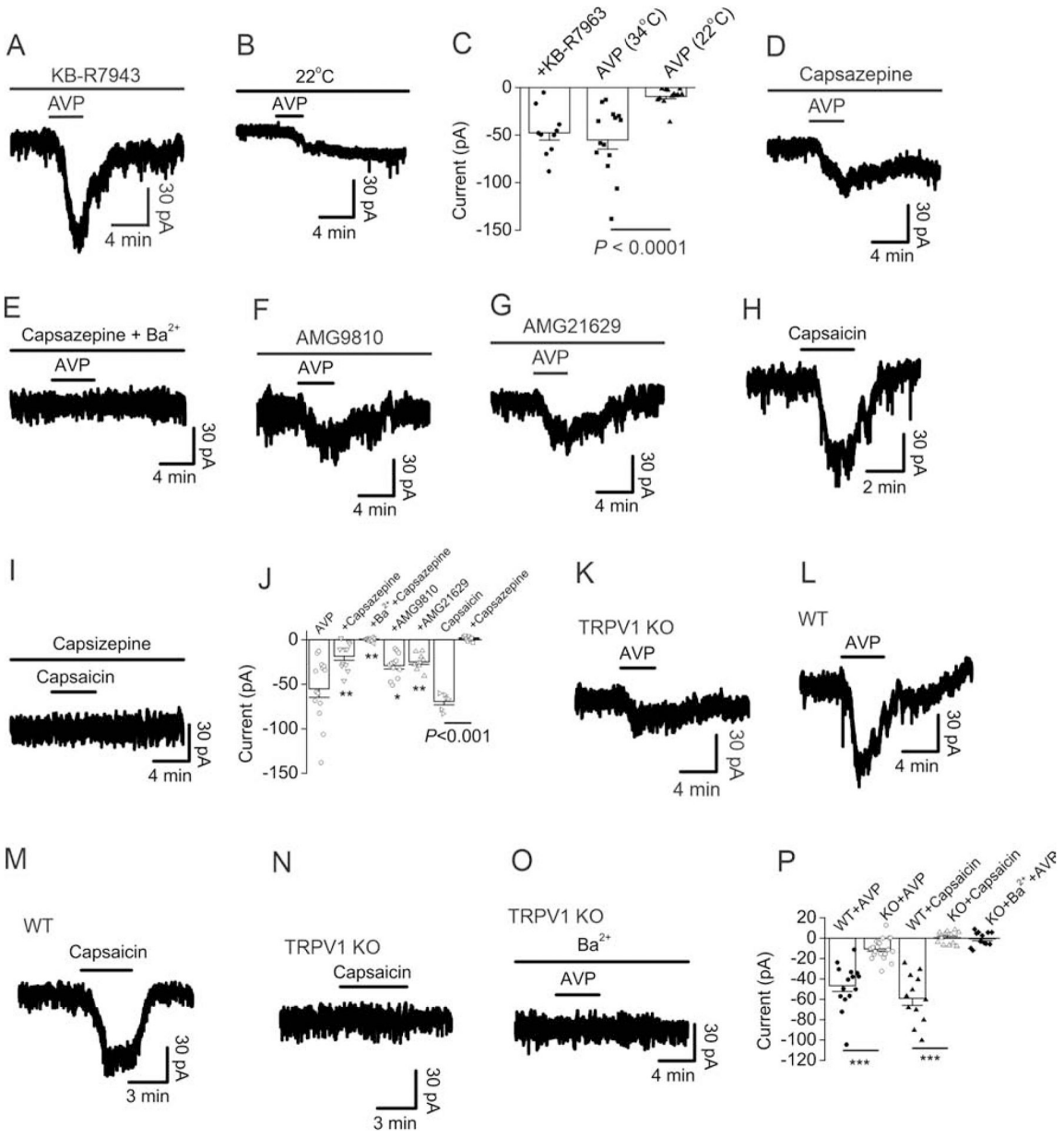

Figure 5. TRPV1 channels are involved in AVP-mediated excitation of subicular pyramidal neurons.

A, Application of the selective Na^+/Ca^{2+} exchanger inhibitor, KB-R7943 (70 μM), did not block AVP-induced inward currents. **B**, Bath application AVP induced a smaller inward current of subicular pyramidal neuron at room temperature (22°C). **C**, Summary graph. **D**, Bath application of the TRPV1 blocker, capsazepine (10 μM), reduced I_{AVP}. **E**, Co-application of the TRPV1 blocker, capsazepine (10 μM) and the Kir channel blocker, Ba^{2+} (300 μM), blocked AVP-elicited inward currents. **F**, Bath application of the selective TRPV1 blocker, AMG9810 (10 μM), reduced I_{AVP}. **G**, Bath application of the selective TRPV1 blocker, AMG21629 (3 μM), reduced I_{AVP}. **H**, Bath application of the TRPV1 agonist, capsaicin (50 μM), evoked an inward current. **I**, Application of the TRPV1 channel blocker,

capsazepine (10 μM), blocked capsaicin-evoked inward currents in a subicular pyramidal neuron. **J**, Summary graph. * $P < 0.05$, ** $P < 0.01$ vs. control I_{AVP}. **K**, Application of AVP induced a small inward current recorded from a subicular pyramidal neuron in a slice cut from a TRPV1 KO mouse. **L**, Application of AVP still evoked a comparable inward current recorded from a subicular pyramidal neuron in a slice cut from a WT mouse. **M**, Bath application of the selective TRPV1 agonist, capsaicin (50 μM), evoked an inward current. **N**, Bath application of capsaicin (50 μM) did not elicit inward currents recorded from a subicular pyramidal neuron in a slice cut from a TRPV1 KO mouse. **O**, Bath application of Ba^{2+} (300 μM) blocked AVP-mediated inward current recorded from a subicular pyramidal neuron in a slice cut from a TRPV1 KO mouse. **P**, Summary graph.

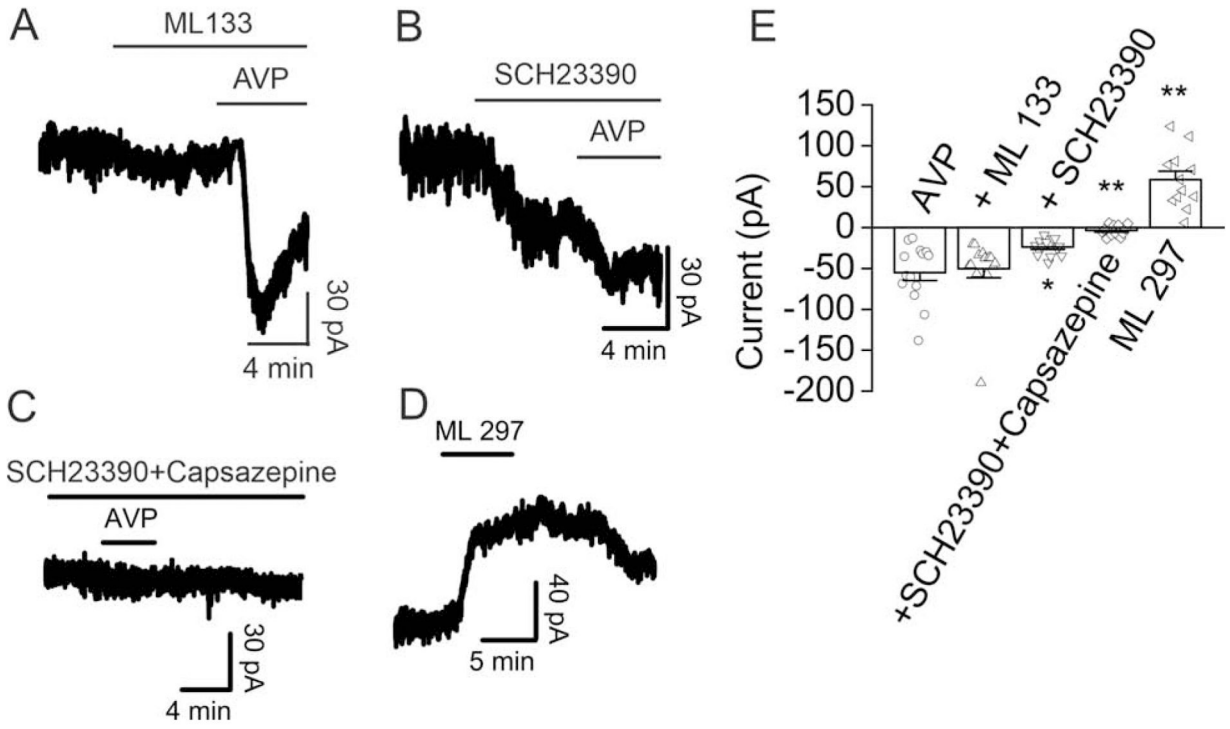

Figure 6. GIRK channels are involved in AVP-elicited excitation of subicular pyramidal neurons.

A, Bath application of the Kir2 subfamily inhibitor, ML 133 (30 μM), did not alter AVP-induced inward current. **B**, Bath application of SCH23390 (20 μM), a GIRK channel blocker, induced an inward current by itself and reduced AVP-elicited inward currents. **C**, Co-application of SCH23390 (20 μM) and the TRPV1 blocker, capsazepine (10 μM) blocked I_{AVP}. **D**, Bath application of ML 297 (10 μM), the GIRK1 activator, induced an outward current. **E**, Summary graph. * $P < 0.05$, ** $P < 0.01$. Empty symbols represented values from individual cells and bar graphs were their averages.

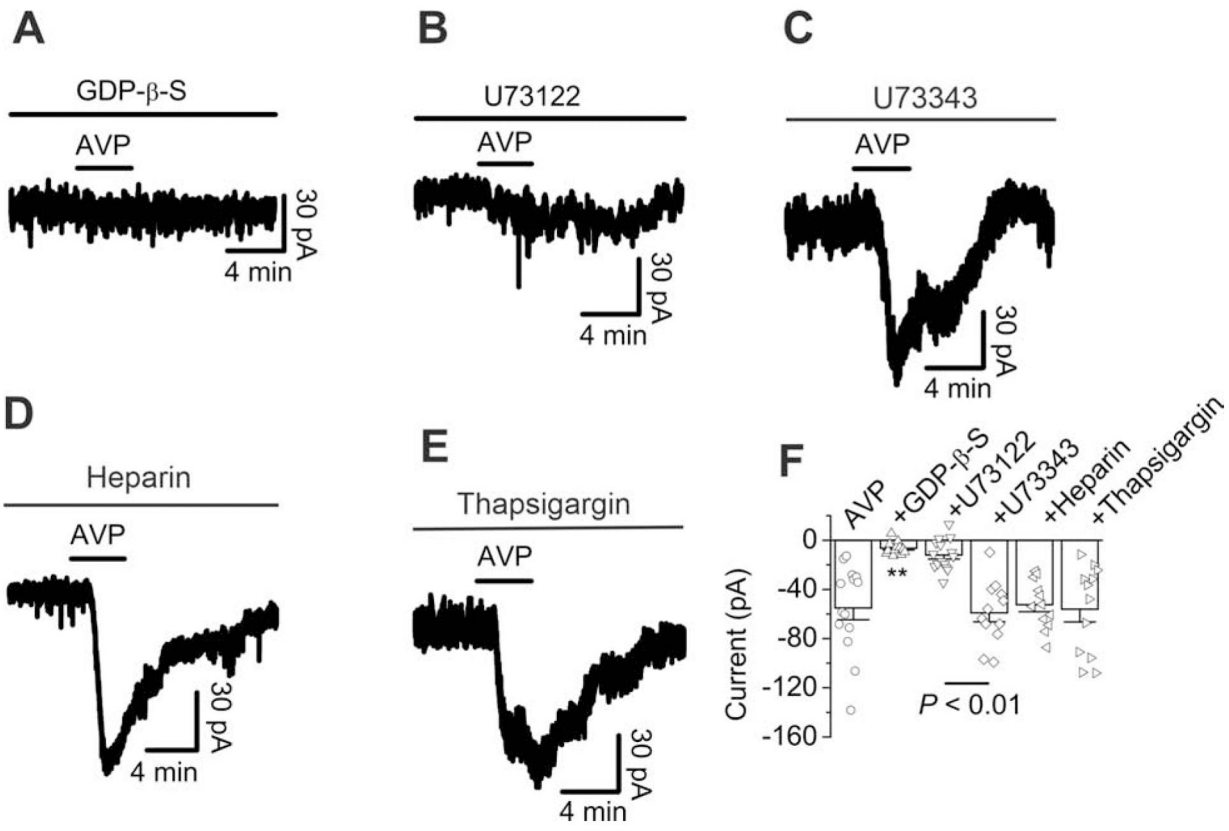

Figure 7. AVP-elicited excitation of subicular pyramidal neurons is dependent on G proteins and PLCβ but independent of intracellular Ca^{2+} release.

A, Intracellular application of GDP-β-S (0.5 mM) via the recording pipettes depressed I_{AVP}. **B**, Pretreatment of slices with U73122 (5 μM) inhibited I_{AVP}. **C**, Pretreatment of slices with the inactive analog, U73343 (5 μM), in the same fashion, did not block I_{AVP}. **D**, Intracellular perfusion of heparin (2 mg/ml) via the recording pipette did not block I_{AVP}. **E**, Intracellular dialysis of thapsigargin (10 μM) did not block I_{AVP}. **F**, Summary graph. Empty symbols were the values from individual cells and bar graphs were their averages. ** $P < 0.01$ vs. control I_{AVP}.

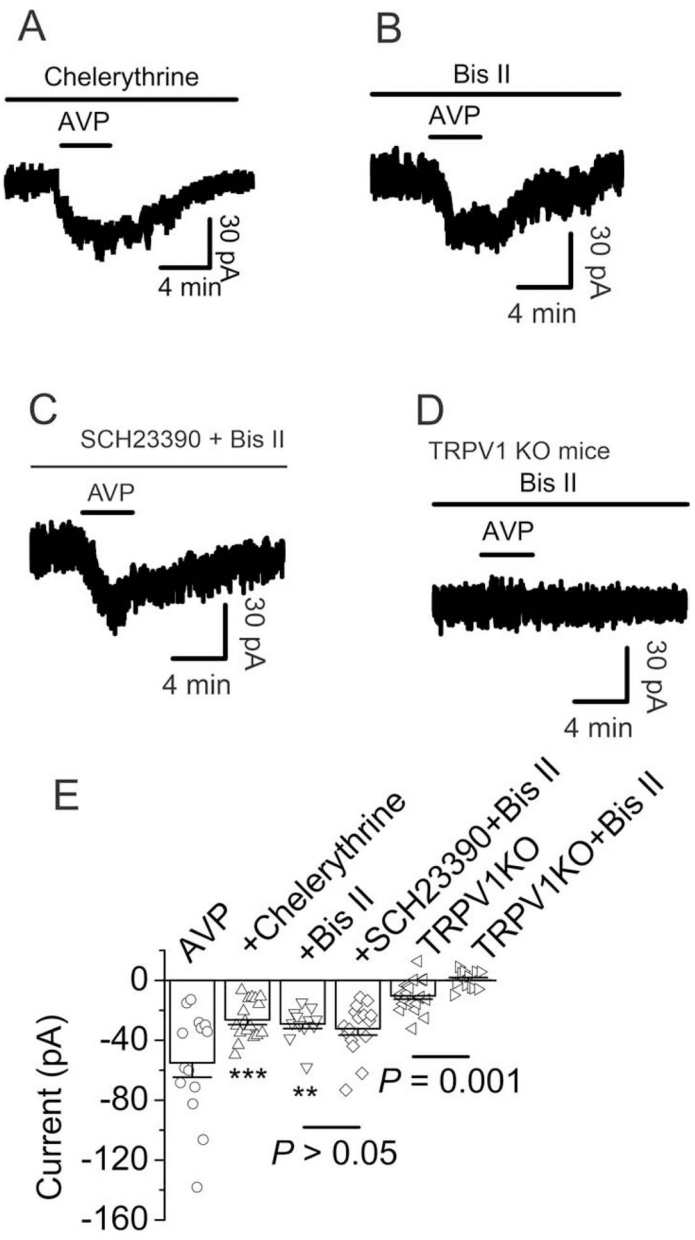

Figure 8. PKC is required for V_{1a} receptor-mediated depression of GIRK channels.

A, Pretreatment slices with and continuous bath application of the selective PKC inhibitor, chelerythrine, reduced AVP-mediated increases in inward currents. **B**, AVP elicited a smaller inward current in slices treated with the selective PKC inhibitor, Bis II. **C**, Blockade of GIRK channels with SCH23390 in the extracellular solution did not alter Bis II-mediated reduction of I_{AVP}. **D**, Treatment of slices with Bis II blocked AVP-induced inward currents in slices cut from TRPV1 KO mice. **E**, Summary graph. ** $P < 0.01$, *** $P < 0.001$ vs. AVP alone.

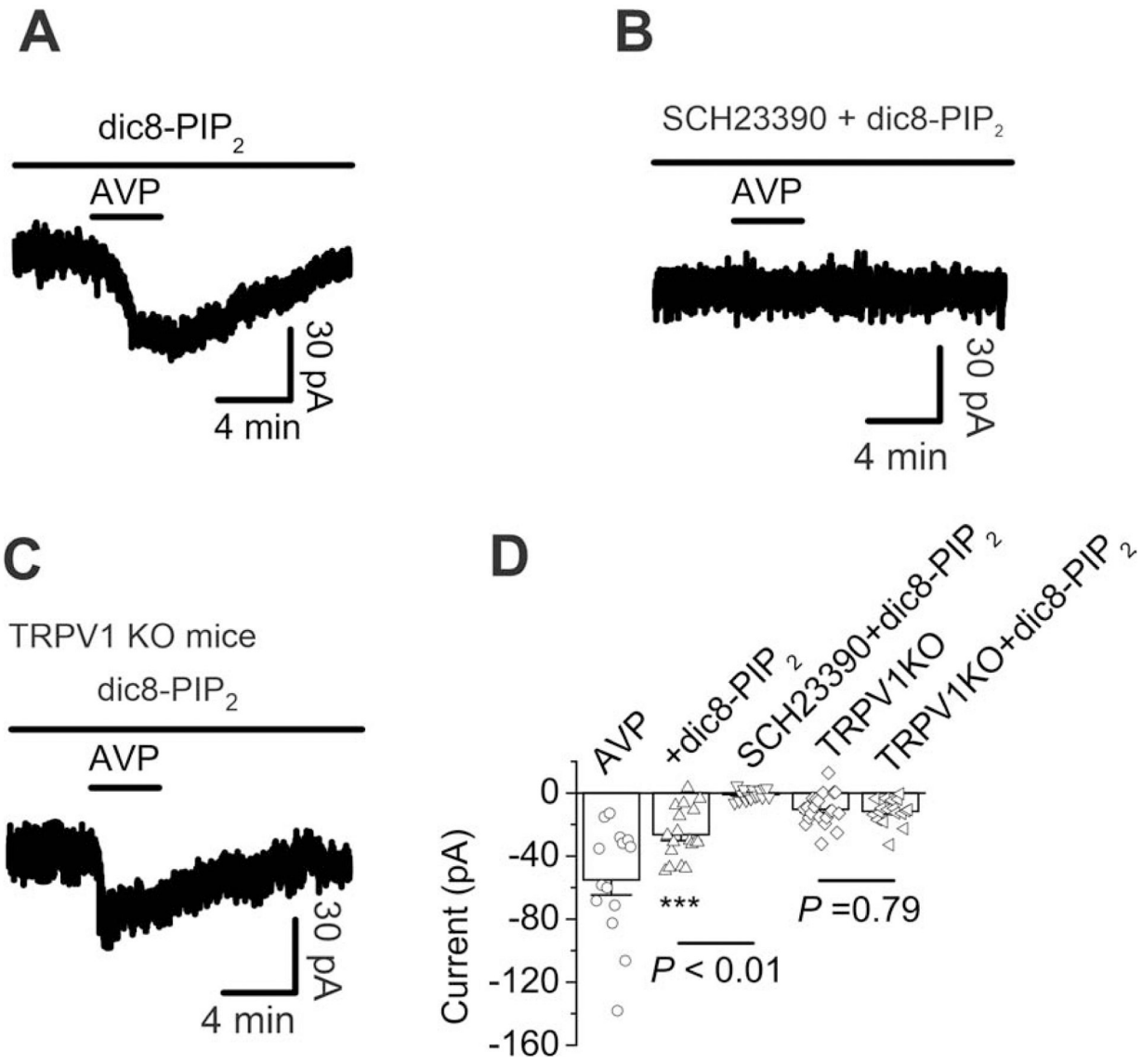

Figure 9. PIP_2 depletion is responsible for V_{1a} receptor-mediated activation of TRPV1 channels.

A, Intracellular perfusion of dic8-PIP_2 reduced AVP-elicited inward currents. **B**, AVP did not induce inward currents in the extracellular solution containing the GIRK channel blocker, SCH23390, and intracellular solution containing dic8-PIP_2. **C**, Intracellular perfusion of dic8-PIP_2 did not change AVP-mediated inward currents in slices cut from TRPV1 KO mice. **D**, Summary graph. *** $P < 0.001$ vs. AVP alone.